

# 2nd Generation Alkaline Electrolysis

---



FORCE Technology

GreenHydrogen.dk.

Technical University of Denmark – Energy Conversion

Technical University of Denmark – Mechanical Engineering

Århus University Business and Social Science – Centre for Energy Technologies (CET (former HIRC))

Final report

EUDP 63011-0200

March 2013

## Content

Content.....	2
1. Introduction.....	4
2. Project Summary and Conclusions .....	5
3. Background and Project Objective .....	10
4. Structure of the report .....	12
4.1. Improved electrodes (WP1).....	12
4.2. Higher operation temperature (WP2).....	12
4.3. Higher operation pressure (WP3).....	12
4.4. Improved electrolysis stacks architecture (WP4).....	13
4.5. Corrosion (WP5) .....	13
4.6. Modular design for easy up scaling (WP6).....	13
4.7. Demonstration (WP7).....	13
5. Improved electrodes (WP 1).....	14
5.1. Track 1 Electrochemical Plating.....	14
5.1.1. Literature study and preliminary experiments.....	14
5.1.2. Electrode development - Processes for producing a stable and durable porous nickel electrode 18	
5.1.3. Electrochemical measurements .....	21
5.1.4. Durability test .....	23
5.1.5. Summary.....	24
5.1.6. References .....	24
5.2. Track 2 Atmospheric Plasma Technology .....	26
5.2.1. Development of improved electrodes (WP 1.1-1.6) .....	26
5.2.2. Manufacturing of electrodes by plasma spraying (WP 1.7) .....	29
5.2.3. Long-term tests and storage of plasma-sprayed electrodes (WP 1.8).....	29
5.2.4. References .....	29
5.3. Track 3 HTP Materials.....	30
5.3.1. Abstract of Frank Allebrod Ph.D. thesis “High temperature and pressure alkaline electrolysis” 30	
5.3.2. Important literature data .....	31
5.3.3. Constructed measurement set-ups.....	35
5.3.4. Specific electrical conductivity measurements on free and immobilized aqueous KOH .....	41

5.3.5.	Alkaline electrolysis cell for 250 °C and 40 bar .....	42
5.3.6.	“Long term” galvanostatic test .....	52
5.3.7.	Summary .....	53
5.3.8.	List of publications of the project from DTU Energy Conversion .....	54
5.4.	Results on improved electrodes .....	54
5.4.1.	Electroplating .....	54
5.4.2.	Atmospheric Plasma Spray .....	55
5.4.3.	HTP electrodes .....	55
5.4.4.	Conclusion .....	56
6.	Higher operation pressure (WP 3) .....	57
7.	Improved electrolysis stack architecture (WP 4) .....	59
8.	Corrosion resistant materials (WP 5) .....	61
9.	Modular design for easy up scaling (WP 6) .....	63
9.1.	Electrolyser module .....	63
9.2.	Deoxer Module .....	64
9.3.	Dryer Module .....	65
9.4.	Water Treatment Module .....	65
9.5.	Power supply and Control unit .....	66
9.6.	Rack Mounted Electrolyser .....	66
10.	Demonstration (WP7) .....	67
10.1.	Building and Installation .....	67
10.2.	Measurement Results .....	68
10.2.1.	Stack efficiency .....	68
10.2.2.	System Efficiency .....	68
10.2.3.	Total production hours .....	68
10.2.4.	Gas purity .....	68
10.2.5.	Cooling .....	69
10.3.	Demonstration .....	69
11.	List of publications .....	70

## 1. Introduction

This report provides the results of the 2<sup>nd</sup> Generation Alkaline Electrolysis project which was initiated in 2008. The project has been conducted from 2009-2012 by a consortium comprising Århus University Business and Social Science – Centre for Energy Technologies (CET (former HIRC)), Technical University of Denmark – Mechanical Engineering (DTU-ME), Technical University of Denmark – Energy Conversion (DTU-EC), FORCE Technology and GreenHydrogen.dk. The project has been supported by EUDP.

Authors and contributors to the project:

- Lars Yde, CET
- Cecilía K. Kjartansdóttir, DTU-ME
- Frank Allebrod, DTU-EC
- Mogens B. Mogensen, DTU-EC
- Per Møller, DTU-ME
- Lisbeth R. Hilbert, FORCE Technology
- Peter Tommy Nielsen, FORCE Technology
- Troels Mathiesen, FORCE Technology
- Jørgen Jensen, GreenHydrogen.dk
- Lars Andersen, GreenHydrogen.dk
- Alexander Dierking, GreenHydrogen.dk

Edited by Anne Nielsen, CET

The overall project administration has been conducted by CET.

## 2. Project Summary and Conclusions

In order to keep production of renewable energy in balance with the consumption load management is needed. Production of hydrogen by water electrolysis can serve as a huge balancing load and at the same time act as an energy storage media.

The overall purpose of this project has been to contribute to this load management by developing a 2<sup>nd</sup> generation of alkaline electrolysis system characterized by being compact, reliable, inexpensive and energy efficient. The specific targets for the project have been to:

- Increase cell efficiency to more than 88% (according to the higher heating value (HHV)) at a current density of 200 mA /cm<sup>2</sup>
- Increase operation temperature to more than 100 degree Celsius to make the cooling energy more valuable
- Obtain an operation pressure more than 30 bar hereby minimizing the need for further compression of hydrogen for storage
- Improve stack architecture decreasing the price of the stack with at least 50%
- Develop a modular design making it easy to customize plants in the size from 20 to 200 kW
- Demonstrating a 20 kW 2<sup>nd</sup> generation stack in H2College at the campus of Århus University in Herning

These targets are well in line with the objectives which were established in the 2009 strategy for RD&D on electrolysis in Denmark for the period 2011-13. The targets for alkaline electrolysis stacks can be summarised as follows:

- Energy efficiency: 88 %
- Cell voltage: 1,68 V
- Current density: 200 mA/cm<sup>2</sup>
- Operation temperature: 100 °C
- Operation pressure: 30 bar

In order to achieve the targets the project has been organised in the following work packages, which roughly creates the structure of this report:

- WP1: Improved electrodes
- WP2: Higher operation temperature
- WP3: Higher operation pressure
- WP4: Improved electrolysis stacks architecture
- WP5: Corrosion
- WP6: Modular design for easy up scaling
- WP7: Demonstration

### *Improved electrodes and elevated operation temperatures (WP1 and 2)*

The project has included research and development on three different technology tracks of electrodes; an electrochemical plating, an atmospheric plasma spray (APS) and finally a high temperature and pressure (HTP) track with operating temperature around 250 °C and pressure around 40 bar. The HTP track was misleadingly named 'the ceramic track' in the initial project description submitted with the EUDP application. The more correct term 'high temperature and pressure track' (HTP) will be used for the rest of this report. Both the electrochemical plating and the HTP track have each involved a PhD study, which is reflected in this report.

The results obtained in WP 1 show that all three electrode tracks have reached high energy efficiencies. In the electrochemical plating track a stack efficiency of 86.5% at a current density of 177mA/cm<sup>2</sup> and a temperature of 74.4 °C has been shown. The APS track showed cell efficiencies of 97%, however, coatings for the anode side still need to be developed. The HTP cell has reached 100 % electric efficiency operating at 1.5 V (the thermoneutral voltage) with a current density of 1.1 A/cm<sup>2</sup>. This track only tested small cells in an externally heated laboratory set-up, and thus the thermal loss to surroundings cannot be given.

Elevation of operation temperature has been a part of the PhD study on HTP electrodes. Literature studies as well as experimental work have shown that elevation of operating temperature causes remarkably higher current density entailing higher cell efficiency.

As the HTP track is still on research level and the elevated temperature combined with the highly corrosive electrolyte KOH require highly resistant materials for the electrodes the elevated temperatures have not been pursued for the other two tracks.

Based on the findings in the project GreenHydrogen.dk has assessed that the electroplating track on the short term gives the most promising performance when combining durability, lifetime, efficiency and production price. This track has been chosen for further development and demonstration in three projects; 'Optimisation of 2nd Generation Alkaline Electrolysis', 'Hyprovide' and 'High-efficiency, low-cost electrode-surfaces for next generation alkaline electrolysis', which respectively pursue optimisation of the production of electrodes and scaling up the electrolysis system to MW size.

### *Higher operation pressure (WP 3)*

The goal set for the 2<sup>nd</sup> generation electrolyser system, has been to generate 30 bar pressure in the cell stack. Water electrolysis generates hydrogen at a very high pressure, which provides the possibility to generate compressed hydrogen directly from the cell stack, without spending additional power on compression afterwards.

Further, high pressure electrolysis offer the advantage of reduced size of tubing and components, which provides a possibility to increase the capacity or reduce the size of the components by a factor equal to the pressure ratio. This enables the electrolyser system to be designed with a significantly smaller footprint than equivalent atmospheric systems.

An obstacle to be overcome has been to ensure equalisation of the H<sub>2</sub> and O<sub>2</sub> pressure to avoid that mixing of gasses can occur. To solve this problem, a special equilibrium valve has been developed to mechanically control that the pressure of the H<sub>2</sub> at all times equals the O<sub>2</sub> side.

The developments in this work package have resulted in a stack design, which is a cylindrical pressure vessel, with each cell having a cell “wall” sufficiently thick, to resist the high pressure and sealed with O-rings for perfect sealing at high pressures. The stack has in test proved to resist a pressure on 45 bar, though some adjustment is still needed to optimize the pressure resistance and efficiency.

#### *Improved electrolysis stack architecture (WP 4)*

The primary goal of WP4 has been to develop an electrolyser stack concept suitable for mass production, while still solving the technical challenges when designing a high pressure alkaline electrolyser stack. The challenges are mechanical strength, electrolyte and gas flow, stray currents and galvanic corrosion.

When deciding on the new stack design both a ‘zero gap’ and ‘non-zero gap’ was considered. The zero gap design is more efficient than non-zero gap, however the design is more complex and very costly, primarily because the additional materials and production costs for zero gap electrodes..

From these considerations, the concept of a “low gap”, low diameter, high pressure and high cell number electrolyser stack was born, which could offer an improved efficiency of the electrolyser without causing the same high material and production cost as a zero gap zero gap solution.

As a result the low gap design and pressurized stack has reduced the price by 60% of the total system, as well as a reduced system footprint.

#### *Corrosion resistant materials (WP 5)*

Hydrogen production at increased temperature, pressure and stack voltage requires that the electrolyser can withstand the aggressive alkaline media under those severe conditions. A design life of more than 10 years is a challenge in terms of materials.

The progress of the project required a special focus on corrosion testing and examination of polymers in order to find alternative durable membrane and gasket materials.

The initial literature survey and the first tests at H2College indicated that the chemical resistance of polymers presented a greater challenge than anticipated, and that test data from commercial suppliers were insufficient to model the conditions in the electrolyser. The alkali resistant polymers (e.g. Teflon) are costly and the search for cheaper alternatives turned into a major aim.

A number of different tests were run under accelerated conditions and the degradation mechanism was examined. The results of standardised tests are summarised in Table 5 on page 61. Consequently, the project has involved corrosion testing and examination of polymers to greater extent than originally planned at the detriment of long-term testing of electrodes (WP 1.8), which has been limited.

Inspiration for the future materials selection in electrolyzers is now available by the combined experience from the experimental work and literature.

### *Modular design for easy up scaling (WP 6)*

One of the strong visions for the 2<sup>nd</sup> generation electrolyser concept has been to develop a modular system with several standardized components, making it possible to deliver a wide range of specification and features to the customer depending on the application. The use of a modular system is also aimed at faster and easier service, by replacing defect modules directly on site to decrease the downtime.

A great effort has been put into analysing the electrolysis system to determine how the different components could be split onto modules. The end result is that following modules have been designed.

- Electrolyser module
- Deozer Module
- Dryer Module
- Water Treatment Module
- Power supply and Control unit
- Rack mount

The goal was to design the electrolysis system to fit into standardized racks, in order to standardize the footprint measurements, and ease installation requirements. This goal was achieved, subsequently the only requirement currently, is available floor space, electricity, water, and pipes for hydrogen, oxygen and ventilation.

### *Demonstration (WP7)*

The developed 2<sup>nd</sup> generation rack-mounted alkaline electrolyser system has been installed and demonstrated for 18 month in a college (H2College) with 66 apartments.

A number of measurements were performed on the system installed in H2College. No measurements on the overall system efficiency were conducted. However measurement on the stack showed a stack efficiency of 86.5% at a current density of 177mA/cm<sup>2</sup> and a temperature of 74.4 °C at the hydrogen outlet.

The system is estimated to have run roughly 2000h during the demonstration period. The demonstration of the 2<sup>nd</sup> generation alkaline electrolyser is considered a success for several reasons. While not all technical goals were reached, the research and development in the project have resulted in some very good solutions for most of the challenges in high pressure alkaline electrolysis.

The concept of a rack mounted electrolyser was proven viable, and all critical aspects of the modularisation have been covered.

The H2College system demonstrates therefor more than the development of a small size electrolyser, it is a leap from developing electrolyser systems as a plant, to developing electrolyser systems as a product suitable for mass production.



### *Dissemination*

The project has generated an extensive amount of significant findings which have been communicated in different ways. Besides having shared main findings from the project within reference groups under the Danish Partnership for Hydrogen and Fuel Cells dissemination have been carried out by publications as articles in international scientific and popular journals as well as presentations and posters on national and international conferences. Further a patent application on the HTP cell has been filed.

For further details on the dissemination activities see chapter 11.

### 3. Background and Project Objective

Energy production from wind turbines is foreseen to constitute a significant part of the future Danish energy sources. A major challenge is however the large variation over time in wind energy production. In order to keep production and consumption in balance load management is needed. Production of hydrogen by water electrolysis can serve as a huge balancing load and at the same time act as an energy storage media.

Electrolysis of water has been used in the industry for decades. Alkaline and to a certain extent PEM electrolysis have been predominant. Characteristics for the alkaline electrolysis have been large systems tailor-made for each plant, non-scalable and with a low efficiency. These systems are so-called 1<sup>st</sup> generation systems.

The objective of this project has been to develop a 2<sup>nd</sup> generation alkaline system characterized by being compact, reliable, inexpensive and energy efficient. The specific targets for the project have been to:

- Increase electrode efficiency to more than 88% at a current density of 200 mA /cm<sup>2</sup>
- Increase operation temperature to more than 100 degree Celsius to make the cooling energy more valuable
- Obtain an operation pressure more than 30 bar hereby minimizing the need for further compression of hydrogen for storage
- Improve stack architecture decreasing the price of the stack with at least 50%
- Develop a modular design making it easy to customize plants in the size from 20 to 200 kW
- Demonstrating a 20 kW 2nd generation stack in H2College at the campus of Århus University in Herning

These targets are well in line with the objectives which were established in the 2009 strategy for RD&D on electrolysis in Denmark for the period 2011-13. The objectives are summarised in the table below:

Tabel 6.1 Sammenfatning af mål og indsatsområder for AEC-indsatsen

	2009-2010	2011-2013	2014-2018
<b>Forskning</b>			
	Elektroder Kraftforsyning (AC-DC) Systemstudier, MW-anlæg Systemstudier, Mikro-anlæg	Elektroder Kraftforsyning (AC-DC) Systemstudier, MW-anlæg	Elektroder Kraftforsyning (AC-DC)
<b>Udvikling</b>			
	Rense og tørre processer Design af elektrolysestak Modulopbygning	Rense og tørre processer Design af elektrolysestak Modulopbygning Mikro-anlæg	Rense og tørre processer Design af elektrolysestak Modulopbygning MW-anlæg
<b>Demonstration</b>			
<b>Stak:</b>	Virkningsgrad: 81 % Cellespænding: 1,82 V Strømtæthed: 100 mA/cm <sup>2</sup> Driftstemperatur: 100 °C Driftstryk: 15 bar	Virkningsgrad: 88 % Cellespænding: 1,68 V Strømtæthed: 200 mA/cm <sup>2</sup> Driftstemperatur: 100 °C Driftstryk: 30 bar	Virkningsgrad: 95 % Cellespænding: 1,56 V Strømtæthed: 400 mA/cm <sup>2</sup> Driftstemperatur: 200 °C Driftstryk: 100 bar
<b>System:</b>	Virkningsgrad, el til brint: 67 % Eflorbrug: 5,2 kW/Nm <sup>3</sup> Virkningsgrad, el til brint +varme: 82 % Varme: 0,780 kWh/Nm <sup>3</sup> brint 30 kW anlæg Modulopbygning	Virkningsgrad, el til brint: 80 % Eflorbrug: 4,4 kW/Nm <sup>3</sup> Virkningsgrad, el til brint +varme: 90 % Varme: 0,453 kWh/Nm <sup>3</sup> brint 30 kW – 300 kW anlæg Mikro-elektrolyseanlæg (10 kW) Modulopbygning	Virkningsgrad, el til brint: 90 % Eflorbrug: 3,9 kW/Nm <sup>3</sup> Virkningsgrad, el til brint +varme: 95 % Varme: 0,175 kWh/Nm <sup>3</sup> brint MW-anlæg Modulopbygning
<b>Reaktionstid:</b>	Systemet reagerer øjeblikkelig	Systemet reagerer øjeblikkelig	Systemet reagerer øjeblikkelig

Table 1: The objectives for the Danish RD&D strategy for electrolysis (*Strategi for Elektrolyse i Danmark, F, U & D 2010-18., 2009, Partnerskabet for Brint og Brændselsceller*)

## 4. Structure of the report

To pursue the targets of the project, different aspects of the electrolysis system has been in focus and divided in seven work packages as outlined below.

### 4.1.Improved electrodes (WP1)

There are two ways to increase the efficiency of an electrode: Increase the specific surface area per unit and thereby get a higher current density or increase the catalytic properties of the electrode surface by which the necessary voltage to draw the current will be lower. The work package will deal with both through literature studies and lab tests in order to find and specify for production the optimal electrode solution regarding efficiency and price.

To pursue the target for the project research will be carried out on three different technologies for manufacturing and surface treatment of electrodes for improving the efficiency:

- Electrochemical plating (DTU-ME)
- Plasma spray with e.g. Raney Nickel at atmospheric pressure by using a protection gas (FORCE)
- HTP cells made by tape casting, silk screen printing or spray painting (DTU-EC)

It is the target of this WP to reach efficiencies of at least 88% at a current density of 200 mA/cm<sup>2</sup>.

### 4.2.Higher operation temperature (WP2)

Most commercial potassium hydroxide water electrolyzers use nickel electrodes and operate at 70-80 °C. Only limited information on electrolyzers operated at elevated temperatures (above 80°C) is available. Increasing the operation temperature for alkaline water electrolysis from the normal 80°C will significantly increase the efficiency. A possible obstacle for operating at elevated temperature is the lower stability of the materials. In this project research of suitable materials for the cell design will be carried out in order to develop the electrolysis plant for operation at elevated temperatures of more than 100 degree Celsius. This topic is closely interconnected to the research carried out by DTU-EC on developing HTP electrodes. Therefore, the results are reported as an integrated part of WP1 in paragraph 5.3 'Track 3 HTP Materials'. (DTU-EC)

### 4.3.Higher operation pressure (WP3)

The energy density of hydrogen is only about 1/3 of that of natural gas. Therefore the produced hydrogen must be compressed to be used as an energy carrier. The hydrogen can be compressed in the electrolyser or by piston compressors. The extra energy consumption used by an electrolyser operated at elevated pressure is quite limited whereas the operation of a compressor is very energy consuming. Therefore it is obvious to develop the 2<sup>nd</sup> generation electrolyser for operation at high pressure in order to reduce or eliminate the demand for further compression. Elevated pressure puts special requirements on the cell frames, gaskets and endplates (GreenHydrogen.dk).

#### **4.4.Improved electrolysis stacks architecture (WP4)**

The electrolyser stack consist of electrodes, membranes, gaskets, ports and manifolds, tie rods and endplates. The work package will deal with the design of the stack in order to find the optimum solution regarding flow of electrolyte, oxygen and hydrogen, corrosion, stray currents, material use, stack volume, suitability for mass production and price reduction. Special attention will be paid to the so-called non zero gap concept by which it might be possible to reduce the price of the stack by a factor of 3 (GreenHydrogen.dk, CET).

#### **4.5.Corrosion (WP5)**

Corrosion in alkaline electrolyzers is a severe problem and increasing with increasing temperature, pressure and stack voltage. In order to secure a lifetime of more than 10 years it is necessary to know and understand the corrosion mechanisms. In this WP analysis and tests in connection with corrosion in hot alkaline environment (corrosion in general as well as stress corrosion etc.) will be carried out. Explanation of corrosion condition and the possibility of hydrogen brittleness as a consequence of hydrogen exposure will be investigated. Material and surface characterizing by use of scanning electron microscope (SEM) and Focused Ion Beam Microscopy (FIB). Fabrication of high pressure cells is not a part of this WP but will be delivered by GreenHydrogen.dk (FORCE, Risø, DTU).

#### **4.6.Modular design for easy up scaling (WP6)**

In order to reduce the engineering for customer design, a modular system will be developed. Modularisation has successfully been used in the UPS industry by American Power Conversion to such extend that the customer literately can design a new UPS system by himself. Experience from the development of this module system will be used (GreenHydrogen.dk).

#### **4.7.Demonstration (WP7)**

Demonstration will take place by substituting a 1<sup>st</sup> generation stack, which is installed at H2College, by the 2<sup>nd</sup> generation stack developed in this project. H2College consists of 66 passive houses at the campus of Århus University in Herning powered by hydrogen made from water and wind power. The plants performance regarding electricity consumption, hydrogen production hydrogen quality, utilisation of cooling energy etc. will be monitored as well as operation experiences will be reported (GreenHydrogen.dk, CET).

## 5. Improved electrodes (WP 1)

Three different tracks of electrode technology have been developed in this project; Electrochemical plating by DTU-ME, Powder Technology by FORCE Technology and HTP material by DTU-EC. The preconditions for each technology are not alike. The electrochemical plating technology has in a PhD study at DTU-ME been refined and developed to obtain an inexpensive method with potential for mass production in the short term. The plasma spray technology, which is a well-known technology, has been developed with the aim to be carried out at atmospheric pressure instead of at vacuum and has further been tested by FORCE Technology. Finally, the third technology, where HTP materials have been used for alkaline electrolysis in order to obtain elevated process temperature, has involved a PhD study as well. This method is still on a research level and as such this technology track was not planned to provide results ready for use at manufacturing level.

The differences in the three tracks regarding involvement of PhD's as well as development level are reflected in the reporting of WP 1 where a common standard for reporting has not been pursued.

### 5.1.Track 1 Electrochemical Plating

#### 5.1.1. Literature study and preliminary experiments

##### *Electrocatalytic activity of the hydrogen electrode*

It has been shown that the best hydrogen electrode is the one having intermediate M – H bond energy (or free energy of hydrogen adsorption ( $\Delta G_{ads}$ ))[1]. When plotting the electrocatalytic activity (exchange current density for hydrogen evolution reaction) vs. the M – H bond strength for different metals a so called volcano plot is formed. The metals that are on the top of the volcano plot are the ones that are the best electrocatalysts for the hydrogen evolution reaction (HER). As seen in Figure 1 platinum has the best electrocatalytic properties for HER. Here after comes rhenium, ruthenium, iridium and silver. However, all these metals are categorised among precious metals and therefore highly expensive. The next metals in the plot are nickel, cobalt and iron. These three metals are therefore possible candidates as raw material for the new hydrogen electrocatalyst to be developed.

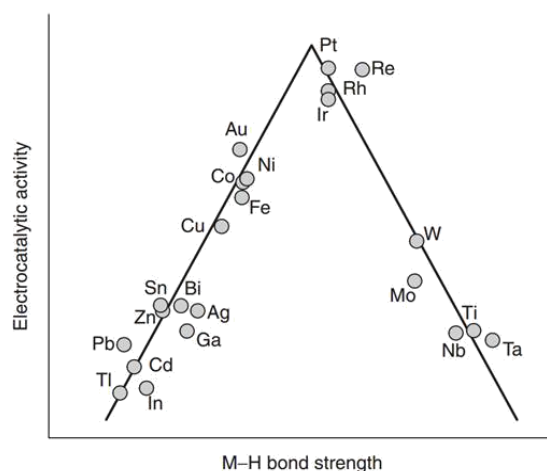
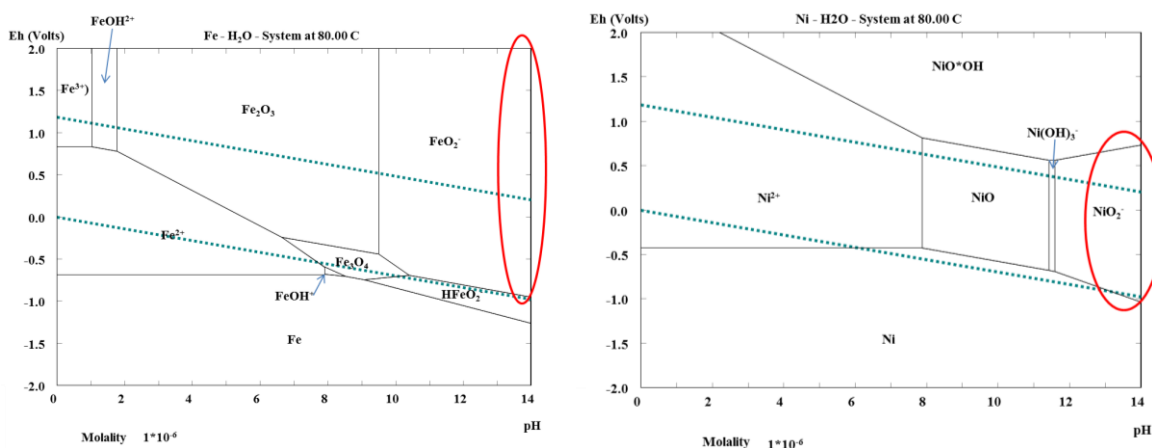


Figure 1: Volcano plot of the electrocatalytic activity for hydrogen evolution reaction vs. metal – hydrogen bond of transition metals [1]

### Corrosion properties

The next step for selecting proper material for the catalyst is to assure that the material is stable, does not corrode, in the operating alkaline media. Pourbaix diagrams are commonly used in chemistry for detecting the thermochemical stable phases of an aqueous electrochemical system. The diagrams are plotted with the pH of the electrolyte on the x-axis and the potential of the metal on the y-axis. Figure 2 shows the calculated Pourbaix diagrams for Iron, Nickel and Cobalt at 80°C and 1 atm. pressure. As the developed electrodes need to be stable in strong alkaline media (pH >14) and at intermediate temperature (> 80). Looking at the calculated diagrams at pH 14 gives an indication of the corrosion resistivity of the metals under the expected electrolysis conditions. Between the two dotted blue lines on the diagrams water is stable. Above the two lines oxygen is stable (oxygen evolution can take place). Whereas, below the two blue lines hydrogen is stable (hydrogen evolution can take place). According to the diagrams, all of the metals decompose at some point inside the -2 to 2 V potential gap. The red circles in Figure 2 indicate at what voltage the decomposition might take place. Fortunately the thermodynamical calculations do not affect the kinetics. That is, they do not tell anything about how fast the metals will corrode or decompose in the particular media.







### *The effect of increasing the surface area*

Electrochemical activity of a catalyst does not only depend on the intrinsic properties of the catalyst. The structure and geometry of a catalyst also have an effect. Platinum black (or platinized platinum) is a good example of this. Platinum black is known to be the ultimate best hydrogen catalyst having zero hydrogen over potential in saturated hydrochloric acid whereas shiny platinum electrode is observed to have 340 mV hydrogen over potential [9]. The reason for the large difference in electrocatalytic activity is that Pt black has a much larger surface area compared to shiny platinum. Although, due to its price, platinum was not considered to be a candidate for the new electrolysis electrode; but its extreme good electrocatalytic properties was an inspiration for the development. In order to learn from the HER “master” Pt surface was produced and its micro structure inspected. Figure 4 shows platinum black surface plated at DTU. The platinum surface appears to be black (Black body) due to the high absorption of all incident electromagnetic radiation, regardless of frequency or angle of incidence. Figure 5 shows images of the platinum surface captured in a high resolution microscope, in two different magnifications. From platinum black we have learned that the electrocatalytic activity of a surface can be largely increased by increasing the real surface area of the catalyst and thus the amount of crystal defects, where the HER is suggested to take place.



Figure 4: Platinum black surface electroplated at DTU

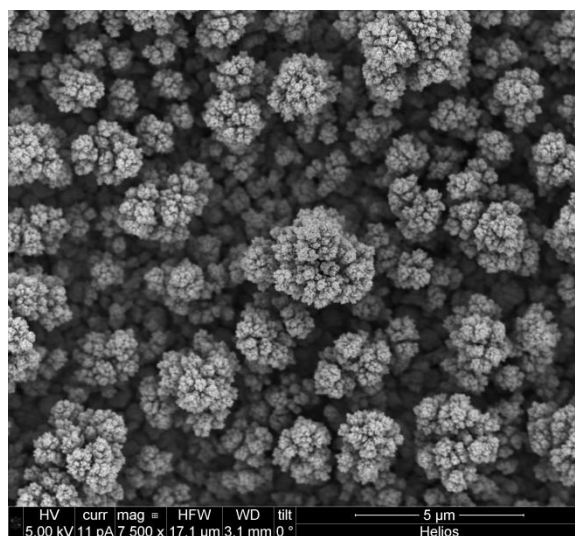
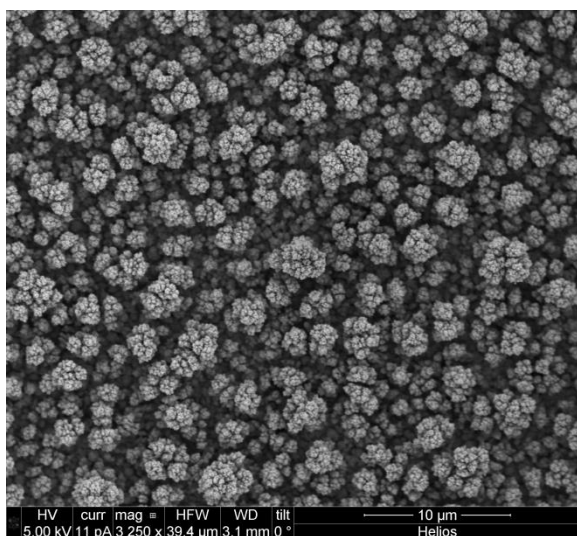


Figure 5: High resolution scanning electron microscope images of Platinum black surface plated at DTU

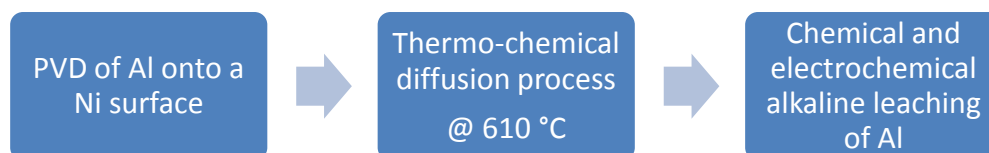
### Production methods

The aim was to produce a nickel surface with large real surface area. Looking into the literature, Justi and Winsel discovered the highly porous Raney nickel as a cathodic electrocatalyst in an alkaline media already in 1961[10]. Raney nickel is mostly prepared by selectively leaching of aluminium from Ni-Al alloys. This process is often referred to as activation. Lattice vacancies formed when leaching causes large surface area and high activity due to very reactive lattice defects[11]. The activated catalysts therefore provide superior performance, compared to smooth nickel cathodes. Plasma spraying or co-depositing nickel alloys ( $\text{NiAl}_3$ ,  $\text{Ni}_2\text{Al}_3$ ) onto a nickel or steel support are common techniques applied when producing Raney nickel electrodes [12]. Cold rolling and hot dipping of aluminium combined with a thermo-chemical diffusion process have also been proposed[13][14]. However, the reproducibility and durability of the Raney nickel electrodes is often deficient[15]. The drawback of the commercial plasma spraying is that relatively brittle nickel phase is formed. Furthermore, the adhesion between the porous surface and the underlying substrate is often poor. From the previous it was clear that new processes for making porous nickel structure that are robust and durable needed to be established.

Magnetron sputtering is a plasma vapour deposition (PVD) process where sputtering material is ejected from a sputter target due to bombardment of ions to a substrate surface. In the particular case the aluminium metal are sputtered to the electrode surface forming a thin film of aluminium. The magnetron sputtering technique can provide superior interlayer adhesion between the substrate and the coated film. Moreover, the thickness of the coated layer can be controlled precisely assuring unique uniformity. Thus, instead of using the typically thermal spraying process to form a porous nickel structure it was decided to select the magnetron sputtering process for depositing an aluminium tinfilm onto a nickel or nickel plated substrate and afterward form the desired Ni/Al alloys with a proper heat treatment.

#### 5.1.2. Electrode development - Processes for producing a stable and durable porous nickel electrode

As for the porous nickel electrodes prepared during this project by PVD process, the effort has mainly been concentrated on coating of commercially pure nickel. For lowering the production cost for large scale production, plating nickel onto an iron or a stainless steel plate would be a better alternative. The process flow for the developed porous nickel plates was as follows.



**Fejl! Henvisningskilde ikke fundet.**, Figure 9 and Figure 10 show images of the developed nickel electrode after Al PVD, heat treatment and leaching, respectively. After alkaline leaching the surface has a black appearance indicating large actual surface area like a black body.



Figure 6 Nickel plate coated with approx. 20  $\mu\text{m}$  of aluminium via Magnetron sputtering is a plasma vapour deposition

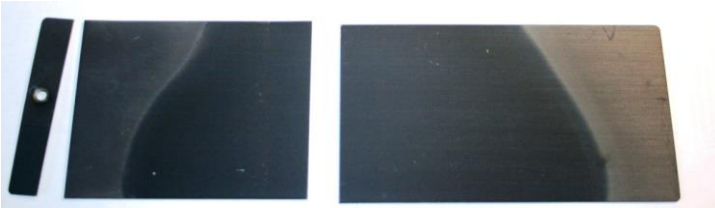


Figure 7 PVD aluminium plated nickel after heat treatment



Figure 8 The PVD aluminium nickel plate after heat treatment and selectively etching of aluminium

The Al PVD was prepared on nickel surface by a non-reactive dc magnetron sputtering at The Danish Technological Institute in Aarhus. During the thermo-chemical diffusion, the aluminium atoms diffuse into the nickel structure and a several intermetallic phases between Al and Ni is formed. The red horizontal line in the phase diagram in Figure 9[16] indicates which Ni-Al diffusion couples are possible at 610  $^{\circ}\text{C}$  and atmospheric pressure. The thickness of each intermetallic phase formed depends on the amount of Ni and Al available in the diffusion system and the heat treatment. The SEM image in Figure 9 shows cross section of a PVD Al/Ni electrode after heat treatment prior etching.

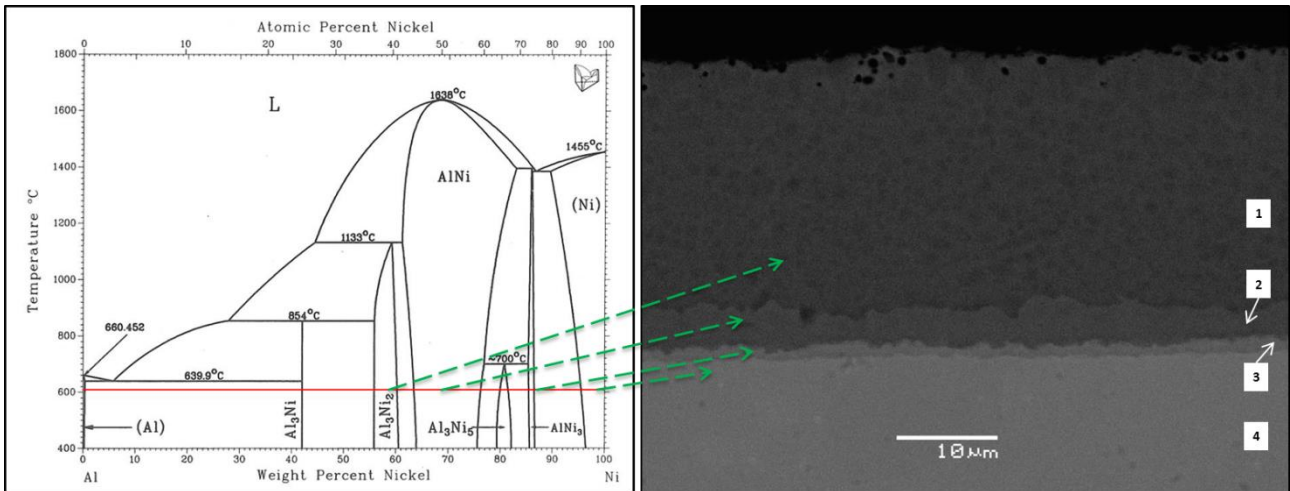


Figure 9: To the left. Phase diagram for the Ni-Al diffusion couples. The red line indicates the thermo-chemical diffusion temperature selected. To the right, cross section SEM image of a PVD Al/Ni electrode after heat treatment at 610 °C. The arrows indicate the type of intermetallic phase in the PVD Al/Ni cross section.

Figure 10 and Figure 11 show cross section microscope images of the PVD Al/Ni electrodes after the heat treatment followed by the first and second alkaline leaching procedure, PVD Al/Ni 1 and PVD Al/Ni 2, respectively. With the first leaching process about 5 μm skeletal Ni/Al residues is formed. When selectively leaching the Al with the second leaching procedure, the entire Al<sub>3</sub>Ni<sub>2</sub> phase is leached, resulting in considerably larger porous nickel layer. The difference is due to optimized leaching procedure.

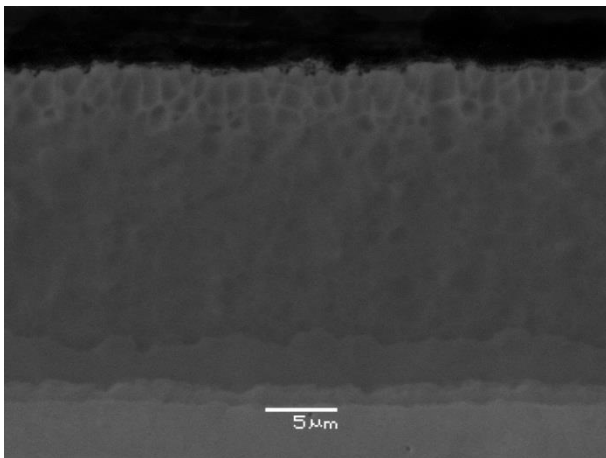


Figure 10: Cross section image of a PVD Al/Ni 1. Electrode prepared by the unoptimized procedure of selectively leaching the aluminium.

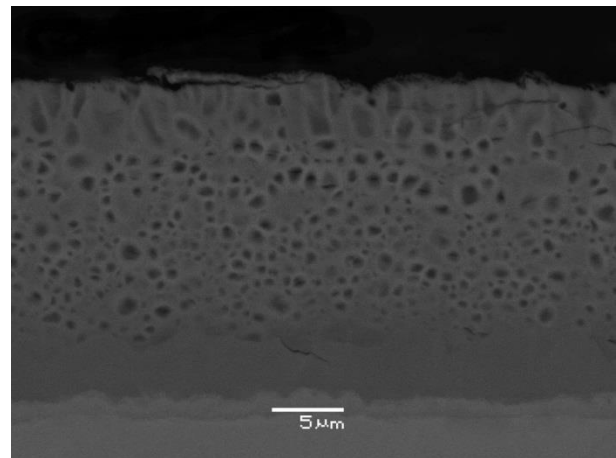


Figure 11: Cross section image of a PVD Al/Ni 2 leached electrode after optimizing the selectively leaching of aluminium.

The cross section images above reveal highly porous nickel microstructure with pores in the range of approximately 0.5-1.5 μm. For nanostructure investigations high resolution microscope studies were required. High resolution microscope images of the PVD Al/Ni 2 specimen surface at two different magnifications are shown in Figure 12. When looking at the image D, where the maximum resolution is reached, 200,000 times magnification, nanopores down to 20 nm can be detected.

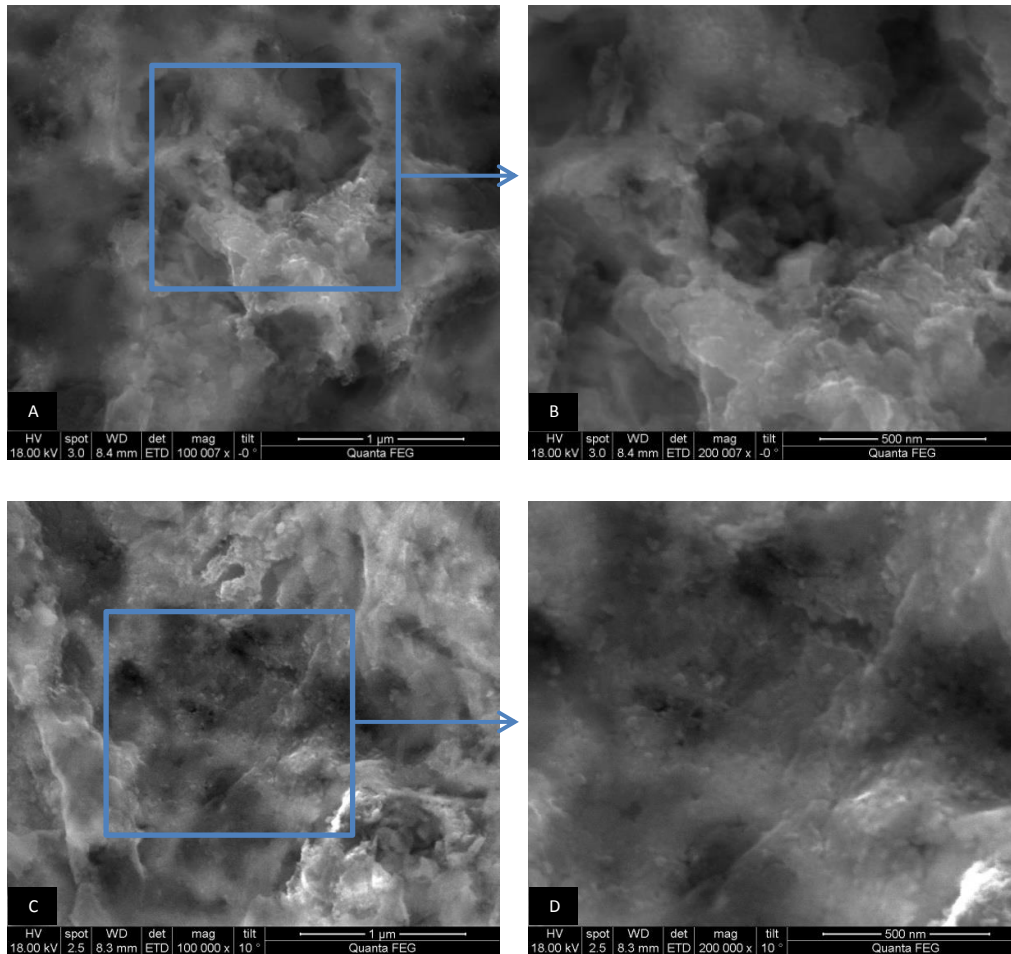


Figure 12: HR-SEM images of the Al PVD Ni 2 surface after heat treatment and optimized alkaline etching of aluminium.

### 5.1.3. Electrochemical measurements

During this project cyclic sweep electrochemical methods have been used for screening of different materials. Simultaneously, the processes capability has been examined. On the basis of the results, it was concluded that the test setup needs to be extremely accurate. This can only be achieved with the right kind of compensation possibilities and a high degree of care when carrying out the experiments. Due to that, a large effort has been put into designing accurate and reliable measurement setups.

Figure 13 shows four cathodic polarisation curves recorded on a PVD Al/Ni 2 surface electrode in 1 M KOH at 25 °C and current densities up to 1.6 V. As seen from the figure, the measurements are consistent. When comparing the polarisation curves with measurements of smooth nickel under the same conditions, also showed in Figure 13, it can be seen that the developed PVD Al/Ni electrodes have 400 mV lower hydrogen over potential compared to a smooth nickel.

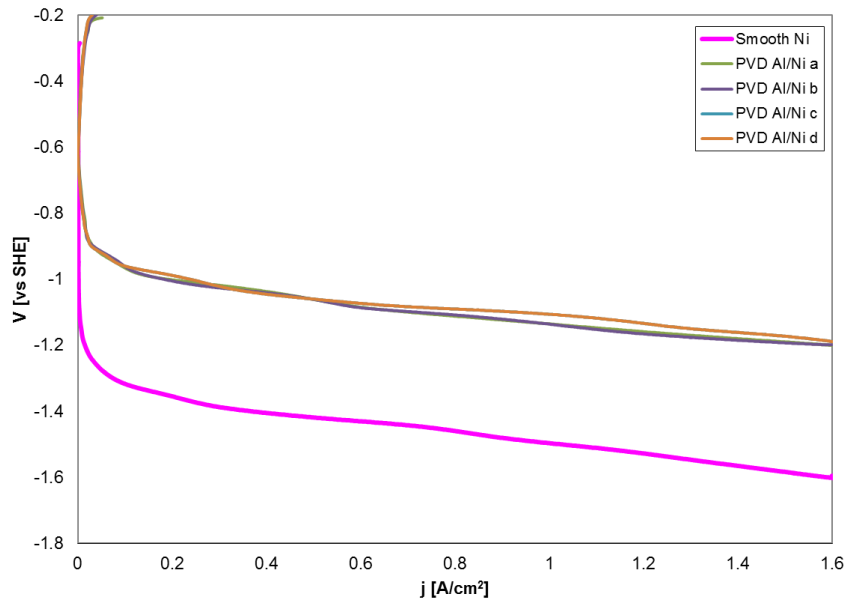


Figure 13: Cathodic polarization curves for PVD Al/Ni 2 repeated 4 times and smooth nickel in 1 M KOH electrolyte at 25 °C.

Figure 14 shows three anodic polarisation curves recorded on a PVD Al/Ni 2 surface. As seen from the figure the developed PVD Al/Ni electrodes have about 50 mV lower oxygen over potential compared to smooth nickel in 1 M KOH at 25 °C at a current up to 0.6 V.

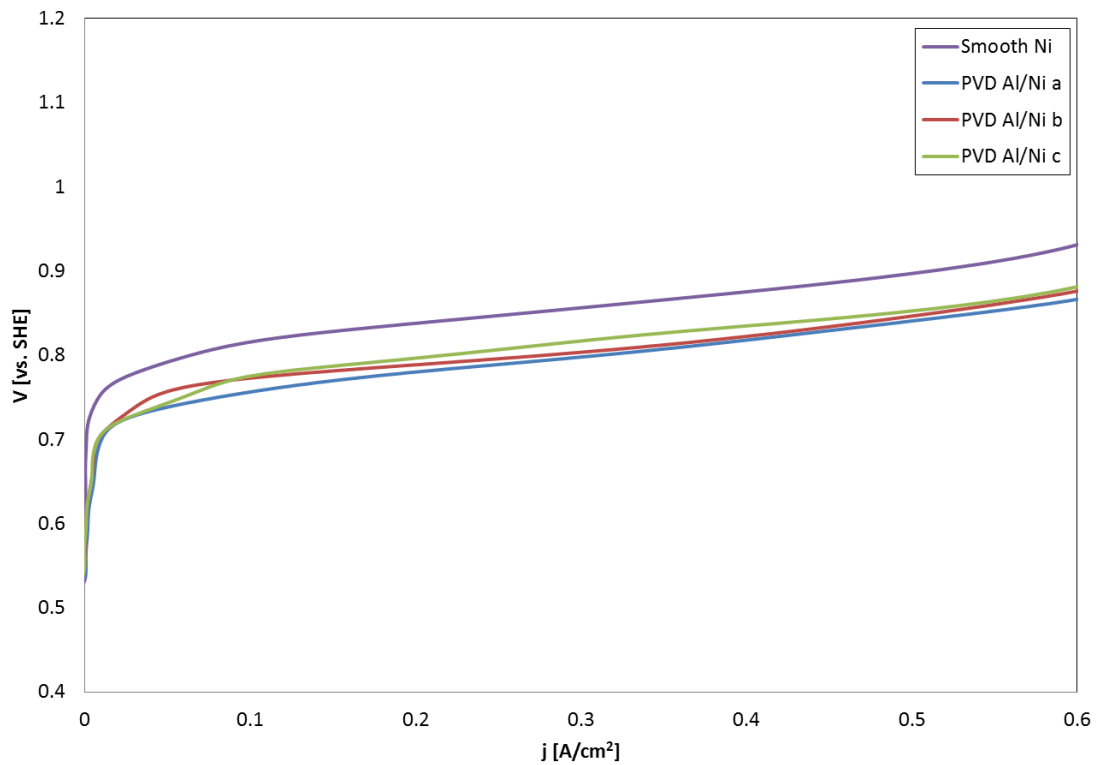


Figure 14: Anodic polarization curves for PVD Al/Ni 2 repeated 3 times and smooth nickel in 1 M KOH electrolyte at 25 °C



Cathodic polarization curves made in 25% KOH at 70 °C are shown in Figure 15. The curves indicate that the PVD Al/Ni 2 is more active towards the hydrogen evolution reaction (HER), compared to PVD Al/Ni 1. This is in agreement with Figure 10 and Figure 11. Namely, that PVD Al/Ni 2 has larger porous nickel residue and thus higher catalytic activity. Compared to smooth nickel, the PVD Al/Ni 1 and PVD Al/Ni 2 have around 220 and 300 mV lower hydrogen over potential at 200 mA/cm<sup>2</sup> in 25% KOH at 70 °C, respectively.

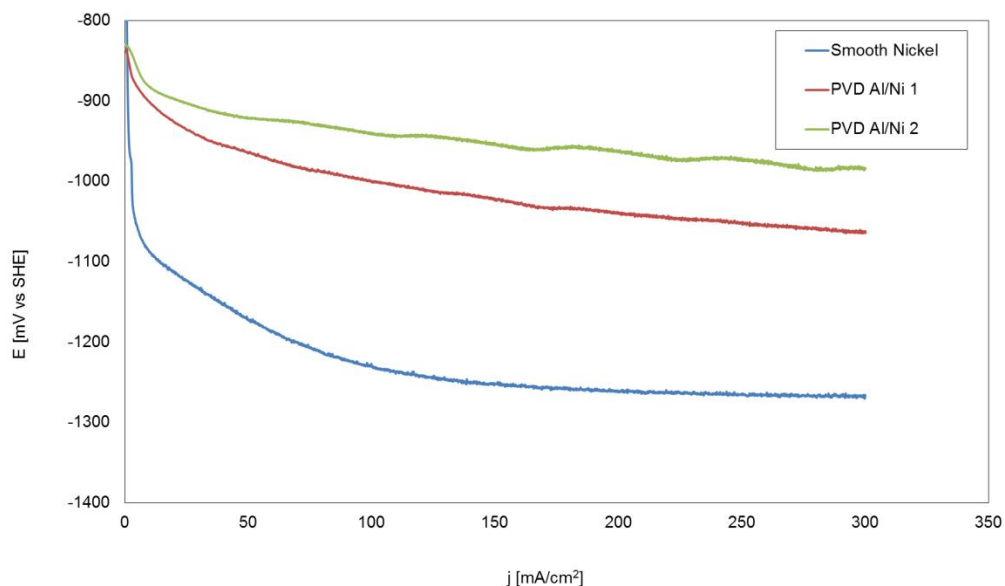


Figure 15: Polarization curves of PVD Al/Ni 1, PVD Al/Ni 2 and blank nickel in 25% KOH electrolyte at 70 °C. Measurements made at FORCE Technology

#### 5.1.4. Durability test

Durability test on sixteen PVD Al/Ni electrodes was carried out in a commercially produced 17-cell bipolar electrolyser from GreenHydrogen.dk. The end plates in the electrolyser were made of pure nickel. The test indicated no serious mitigation in the electrode efficiency during the 9000 hour testing period. The efficiency of the electrolysis stack was measured to be around 78-79 % compared to the higher heating value (HHV) at 65 °C. It should be mentioned that the electrolysis stack was of an old version and some efficiency loss was caused by the stack itself and not by the electrodes. Furthermore, the first and last electrodes in the stack were made of pure nickel. Figure 16 shows efficiency measurements made on the stack at 22 atm. pressure and 200 mA/cm<sup>2</sup> current density.

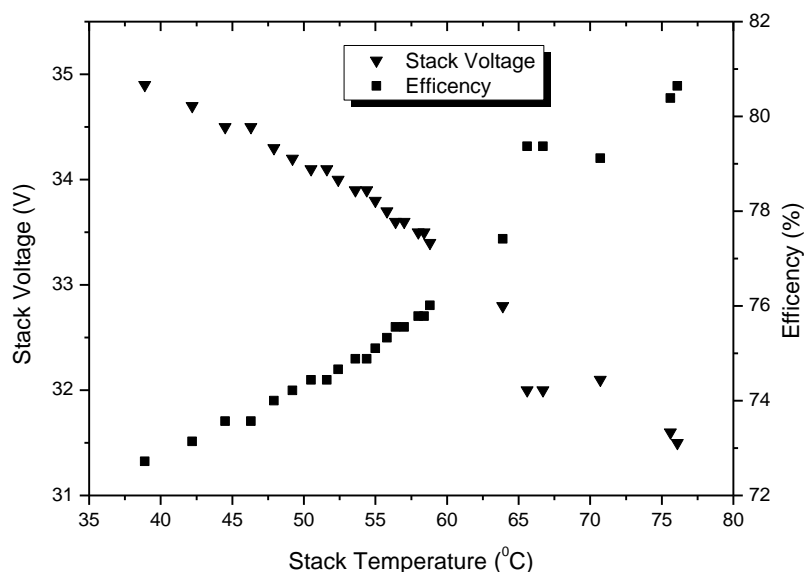


Figure 16: Efficiency measurement made on a 17-cell bipolar electrolysis stack containing 16 electrodes with the developed electrocatalytic surface. The efficiency measurements were made after more than 9,000 operation hours at 22 bars and 200 mA/cm<sup>2</sup> current density.

### 5.1.5. Summary

During the presented Ph.D. study, a new type of electrodes, suitable for industrial alkaline water electrolyzers, has been developed. The electrodes are produced by magnetron sputtering a thin film of aluminium onto a nickel or nickel plated substrate. Hereafter, the aluminium is interdiffused into the nickel surface, by heating, and several intermetallic phases between Al and Ni are formed. Lastly, aluminium is selectively leached from one of the intermetallic phases on the surface and high porous nickel electrode is formed.

The structure of the developed electrodes has been characterised via high resolution scanning electron microscopes, revealing large actual surface area with pores down to 20 nm. Consistent electrochemical measurements show that the developed electrodes need 450 mV less voltage for decomposing water into hydrogen and oxygen compared to smooth nickel electrodes, in 1 M KOH at 25 °C and 1 atm. durability test in an electrolysis stack for 9,000 hours indicate no mitigation in the electrochemical efficiency of the electrodes.

### 5.1.6. References

- [1] S. Trasatti, "ELECTROCHEMICAL THEORY | Hydrogen Evolution," in *Encyclopedia of Electrochemical Power Sources*, Editor-in-Chief: Jürgen Garche, Ed. Amsterdam: Elsevier, 2009, pp. 41–48.
- [2] C. K. Dyer, "Improved Nickel Anodes for Industrial Water Electrolyzers," *J. Electrochem. Soc.*, vol. 132, no. 1, pp. 64–67, Jan. 1985.



- [3] H. Wendt, H. Hofmann, and V. Plzak, "Materials research and development of electrocatalysts for alkaline water electrolysis," *Materials Chemistry and Physics*, vol. 22, no. 1–2, pp. 27–49, 1989.
- [4] S. P. Singh, R. N. Singh, G. Poilleurat, and P. Chartier, "Physicochemical and electrochemical characterization of active films of LaNiO<sub>3</sub> for use as anode in alkaline water electrolysis," *International Journal of Hydrogen Energy*, vol. 20, no. 3, pp. 203–210, Mar. 1995.
- [5] H.-K. Lee, E.-E. Jung, and J.-S. Lee, "Enhancement of catalytic activity of Raney nickel by cobalt addition," *Materials Chemistry and Physics*, vol. 55, no. 2, pp. 89–93, 1998.
- [6] M. El Baydi, S. K. Tiwari, R. N. Singh, J.-L. Rehspringer, P. Chartier, J. F. Koenig, and G. Poilleurat, "High Specific Surface Area Nickel Mixed Oxide Powders LaNiO<sub>3</sub> (Perovskite) and NiCo<sub>2</sub>O<sub>4</sub> (Spinel) via Sol-Gel Type Routes for Oxygen Electrocatalysis in Alkaline Media," *Journal of Solid State Chemistry*, vol. 116, no. 1, pp. 157–169, Apr. 1995.
- [7] M. Merrill and R. Dougherty, "Metal oxide catalysts for the evolution of O<sub>2</sub> from H<sub>2</sub>O," *JOURNAL OF PHYSICAL CHEMISTRY C*, vol. 112, no. 10, pp. 3655–3666, Mar. 2008.
- [8] J. O. Bockris and T. Otagawa, "The Electrocatalysis of Oxygen Evolution on Perovskites," *J. Electrochem. Soc.*, vol. 131, no. 2, pp. 290–302, Feb. 1984.
- [9] D. J. G. Ives and G. J. Janz, *Reference electrodes, theory and practice*. Academic Press, 1961.
- [10] G. Hoogers, in *Fuel Cell Technology Handbook*, Taylor & Francis, 2002.
- [11] V. S. Bagotsky, in *Fuel Cells: Problems and Solutions*, John Wiley & Sons, 2012, pp. 209–210.
- [12] H. Wendt and G. Kreysa, *Electrochemical Engineering: Science and Technology in Chemical and Other Industries*. Springer, 1999.
- [13] "Method of producing finely-divided nickel," U.S. Patent 162819010-May-1927.
- [14] T. Boruciński, S. Rausch, and H. Wendt, "Raney nickel activated H<sub>2</sub>-cathodes Part II: Correlation of morphology and effective catalytic activity of Raney-nickel coated cathodes," *J Appl Electrochem*, vol. 22, no. 11, pp. 1031–1038, Nov. 1992.
- [15] R. H. Jones and G. J. Thomas, Eds., in *Materials for the Hydrogen Economy*, 1st ed., 39: CRC Press, 2007.
- [16] T. B. . B., Hugh; Bennett, L.H.; Murray, Joanne L. Massalski, in *Binary Alloy Phase Diagrams. Volumes 1 & 2. TWO VOLUME SET, 2 VOLUME SET*; 1st ed., American Society for Metals, 1986, p. 142.

## 5.2. Track 2 Atmospheric Plasma Technology

The activities at FORCE Technology (FT) have mainly focussed on developing new highly efficient Raney nickel (NiAl) electrode coatings by use of atmospheric plasma spraying (APS). Such electrodes have previously been produced by vacuum plasma spraying (VPS) /1-2/, but the APS technique represents a much simpler and cheaper approach that possibly makes it suitable for large-scale production.

Secondly, FORCE Technology's efforts have involved electrochemical and metallographic characterisation of the electrode coatings produced by APS. This allowed selection and optimisation of the APS coatings before they were produced in larger scale for the demo cell stacks at GreenHydrogen /3/.

WP 1.1-1.6 Iterative improvements of electrodes produced by APS to achieve 88 % efficiency

WP 1.7 Manufacturing of electrodes by plasma spraying

WP 1.8 Long-term tests and storage of plasma-sprayed electrodes

It was shown quite early in the project that highly efficient cathode coatings meeting the goal of 88 % efficiency could be produced by APS. At the same time, FORCE Technology established a test concept for characterising the electrode coatings that verified APS coatings as fully comparable or better than those described in the literature. Both efforts placed the project right on track from the beginning.

Further developments of the APS coatings led to additional improvements in stability of substrate, adhesion to substrate, spraying parameters and optimisation of coating thickness.

Larger electrodes in many shapes and geometries were provided for the pilot test stacks and the results were promising. The electrodes had significantly optimized mechanical and electrochemical properties, compared to the baseline.

Near the end of year two, only marginal improvements were made of the NiAl coatings for the cathode. At this stage, the cathode side was considered nearly or fully developed as evidenced by the impressive efficiency reported for the pilot cells (97 %). The subsequent development of coatings for the anode side did not provide the desired results, but gained important insight about possible future process routes.

Today, the developed NiAl electrodes produced by APS are considered suitable for large-scale production. It is just a matter of demand before the process can be financially attractive. This will require investments and establishment of a company outside FORCE Technology's auspices.

Details about the studies performed by FORCE Technology have been published in a separate report /4/.

### 5.2.1. Development of improved electrodes (WP 1.1-1.6)

The development of APS NiAl coatings has included iterative loops of production, testing and evaluation. In total, approx. 35 batches of test materials have been produced.

The parameters that have been examined include:

- Powder supplies and pre-mixing.
- Addition of alloying elements (e.g.  $\text{Co}_3\text{O}_4$ ).
- Spraying parameters (on-line optimisation by plume analysis).
- Coating thickness.
- Substrate preparation and shapes.
- Final heat treatment.

Most of the materials have been characterised by electrochemical testing and metallographic examination.

Figure 17 shows a comparison of the hydrogen evolution potential at different current densities, i.e. the cathode performance. Compared with non-coated nickel, the NiAl coatings produced by FORCE Technology (APS) provide a considerable improvement (i.e. reduction) in cell voltage, even at a small coating thickness of  $30\ \mu\text{m}$ . The best performance is observed for NiAl  $100\ \mu\text{m}$ . Compared with vacuum plasma spraying (Schiller et al.) and galvanic plating techniques, the APS technique provides better performance as cathode material.

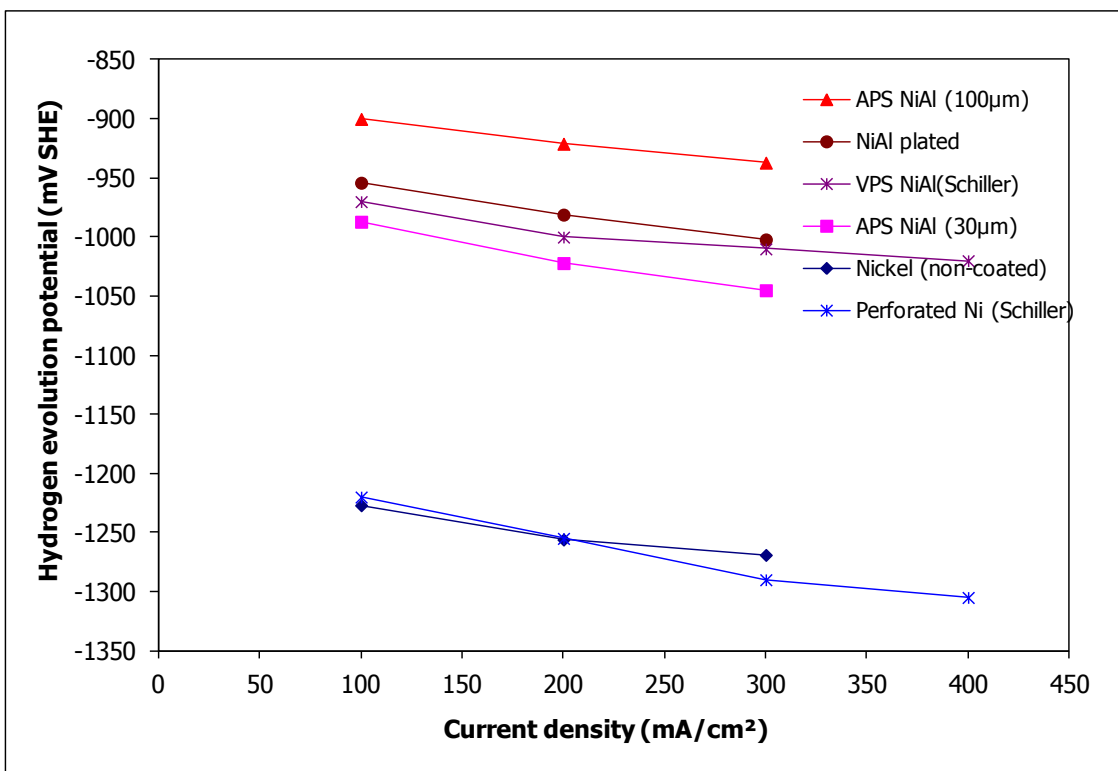


Figure 17. Comparison of cathode potentials at different current densities. Less numeric value means less overvoltage of the hydrogen electrode, i.e. higher efficiency

Figure 18 shows a comparison of the oxygen evolution potential at different current densities, i.e. the anode performance. NiAl coatings produced by APS provide a considerable improvement when compared with the reference material, non-coated nickel. However, the improvement is not as evident as for the cathode side. Alloying with oxides like cobalt oxide ( $\text{Co}_3\text{O}_4$ ) is necessary to obtain further improvement as demonstrated by Schiller, who used VPS. The first attempts using APS did not provide improvement

compared to the NiAl 100  $\mu\text{m}$  coating. Consequently, further research is needed to adapt the APS technique for producing highly efficient anode coatings.

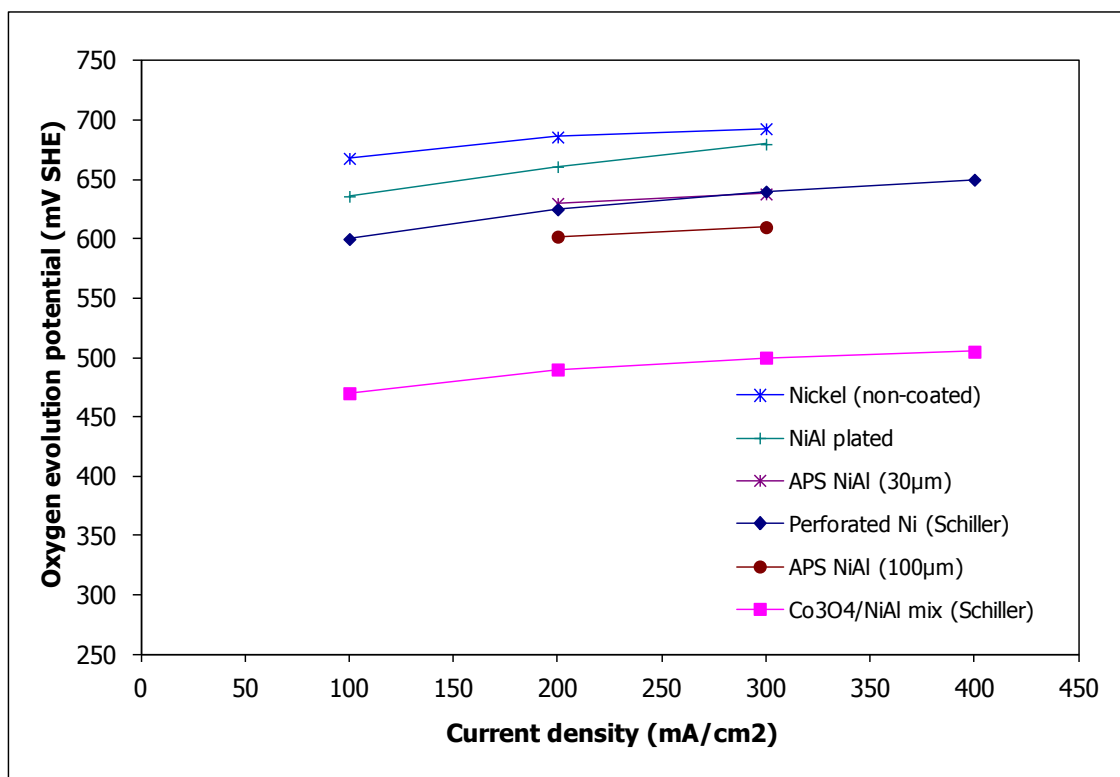


Figure 18. Comparison of anode potentials at different current densities. Less numeric value means less overvoltage of the oxygen electrode, i.e. higher efficiency

The results presented above are based on half-cells measurements of the cathode and anode from which the cell voltage is calculated. Guiding values of the efficiency has then been calculated by using the thermo neutral voltage (1.48 V) as shown in Table 2. The calculated efficiency should be considered the highest attainable in a cell without IR drop. When the coatings are installed in real electrolyzers, the efficiency will be slightly lower, depending on the IR drop in the cell's electrolyte and membrane. However, it is clear that a considerable improvement has been achieved with the new APS NiAl coatings, and similar results can be expected when implementing in electrolyzers as already demonstrated by GreenHydrogen.dk /3/.

	Cell Voltage (V)				Efficiency
	n=1	n=2	avg		
Nickel (non-coated)	1.975	1.940	1.958	76 %	
NiAl (30 $\mu\text{m}$ )	1.683	1.682	1.683	88 %	
NiAl (100 $\mu\text{m}$ )	1.558	1.534	1.546	96 %	
NiAl (300 $\mu\text{m}$ )	1.544	1.548	1.546	96 %	

Table 2: Guiding efficiency of NiAl coatings based on thermo neutral voltage (1.48 V). Non-coated nickel is considered as reference.

### 5.2.2. Manufacturing of electrodes by plasma spraying (WP 1.7)

The systematic screening of Atmospheric Plasma Spraying parameters using a plume analyser combined with analysis of bond strength, pre-treatment and stand-off resulted in un-deformed 0.5 mm nickel plates with a surface area equivalent to 600 cm<sup>2</sup>. The bond strength of the coating was defined as minimum 57 MPa, when not activated. Furthermore, the NiAl consumption was reduced by 74 %.

A major problem was the tension induced by blasting, which was released under the coating process and caused extensive deformation. A method of applying sufficient surface roughness to substrate with minimal adding of tension and deformation was examined. The study suggested that the best results were obtained by combining annealing and sandblasting, when the objectives were minimum deformation and maximum adhesion. However sanding could be sufficient when mesh metal, as the substrate, was to be coated. The applied tensions in the mesh metal are more easily released without causing deformation.

The abovementioned practical problems related to manufacturing NiAl coatings by APS have been identified and solved during the project. The gained experience may be transferred to other cost-effective systems that are cheaper than the nickel substrates used in the project till now.

### 5.2.3. Long-term tests and storage of plasma-sprayed electrodes (WP 1.8)

This work package was scaled down due to higher priority of other activities, i.e. testing of polymer materials. A few tests have been carried out, mainly to evaluate requirements for storage/handling and long-term behaviour of NiAl electrodes.

In most cases, the cathode efficiency decreased while the anode efficiency was unaffected after storing NiAl coatings for long time. Air and water seem as a better medium for storage than KOH. NiAl coatings are fragile and conditioning is decisive for the performance. This is believed to have caused larger spread in the results. The study indicated that procedures for handling and conditioning of NiAl coatings are more crucial than the actual storage media.

The obtained results of extended polarisation of NiAl coatings at -200 mA/cm<sup>2</sup> were not conclusive. In one case, a large decrease is observed in cathode performance over time while another specimen showed good performance. Further refinement of the lab test method is required to obtain consistent results. Promising results on long-term performance of selected APS NiAl coatings have been obtained in pilot cell stacks at GreenHydrogen /3/.

### 5.2.4. References

1. Schiller, G. Henne, R. Mohr, P. and Peinecke, V., High Performance Electrodes for an Advanced Intermittently Operated 10-kW Alkaline Electrolyser, Int. J. Hydrogen Energy, Vol. 23, No. 9, pp. 761-765, 1998.
2. Schiller, G. Henne, R. and Borck, V., Vacuum Plasma spraying of High-Performance Electrodes for Alkaline Water electrolysis, JTTEE5, Vol. 4, No. 2, pp. 185-194, 1995.
3. Final Report, Second Generation Alkaline Electrolysis, EUDP08-II, GreenHydrogen.
4. Troels Mathiesen, Peter Tommy Nielsen and Lisbeth R. Hilbert; Second Generation Alkaline Electrolysis, Final Report of FORCE Technology, 109-22486/TRM & 109-22502/PTN, 29 June 2012.

## 5.3.Track 3 HTP Materials

### 5.3.1. Abstract of Frank Allebrod Ph.D. thesis “High temperature and pressure alkaline electrolysis”

Alkaline electrolyzers have proven to operate reliable for decades on a large scale (up to 160 MW), but in order to become commercially attractive and compete against conventional technologies for hydrogen production, such as natural gas reforming, the production and investment costs have to be reduced. A reduction of the investment costs may be achieved by increasing the operational pressure and temperature of the electrolyser, as this will result in: 1) production of pressurized hydrogen and oxygen, 2) improved electrical efficiencies and 3) increased current density, i.e. increased hydrogen production rate for a given electrolyser cell area.

This thesis describes an exploratory technical study mainly in order to examine the possibility to produce hydrogen and oxygen with a new type of alkaline electrolysis cell at high temperatures and pressures. To perform measurements under high pressure and at elevated temperatures it was necessary to build a measurement system around an autoclave, which could stand high temperatures up to 250 °C and pressures up to 95 bar as well as extremely caustic environments. Based on a literature study to identify resistant materials for these conditions, Inconel 600 was selected among the metals which are available for autoclave construction. An initial single atmosphere high temperature and pressure measurement setup was build comprising this autoclave. A second high temperature and pressure measurement setup was build based on experiences from the first setup in order to perform automatized measurements.

The conductivity of aqueous KOH at elevated temperatures and high concentrations was investigated using the van der Pauw method in combination with electrochemical impedance spectroscopy (EIS). Conductivity values as high as 2.7 S cm<sup>-1</sup> for 35 wt%, 2.9 S cm<sup>-1</sup> for 45 wt%, and 2.8 S cm<sup>-1</sup> for 55 wt% concentrated aqueous solutions were measured at 200 °C. The conductivity of immobilized KOH was determined by the same method in the same temperature and concentration range. Conductivity values as high as 0.67 S cm<sup>-1</sup> for 35 wt%, 0.84 S cm<sup>-1</sup> for 45 wt%, and 0.73 S cm<sup>-1</sup> for 55 wt% concentrated immobilized aqueous solutions were determined at 200 °C.

A new type of an alkaline electrolysis cell was developed in order to operate at high temperatures and pressures. Aqueous potassium hydroxide immobilized electrolyte in porous SrTiO<sub>3</sub> was used in those cells. Electrolysis cells with metal foam based gas diffusion electrodes and immobilized electrolyte were successfully demonstrated at temperatures up to 250 °C and 40 bar. Different electro-catalysts were tested in order to reduce the oxygen and hydrogen overpotentials. Current densities of 1.1 A cm<sup>-2</sup> and 2.3 A cm<sup>-2</sup> have been measured at a cell voltage of 1.5 V and 1.75 V, respectively, without using expensive noble metal catalysts. Electrical efficiencies of almost 99 % at 1.1 A cm<sup>-2</sup> and 85 % at 2.3 A cm<sup>-2</sup> combined with relatively small production costs may lead to both reduced investment and operating costs for hydrogen and oxygen production. One of the produced electrolysis cells was operated for 350 h. Based on the successful results a patent application covering this novel cell was filed. Assuming that the developed cells will be scaled up and successfully tested for some thousand hours, they may offer an important role in future energy storage scenarios.

### 5.3.2. Important literature data

#### *Thermodynamics of water splitting*

There are significant advantages of performing water or steam electrolysis at elevated temperature. The following section describes how the reversible cell voltage and the thermo-neutral voltage behave as a function of temperature and pressure. Furthermore, methods to calculate these potentials are given that make it possible to calculate those without the necessity to use steam tables.

The thermo-neutral voltage  $E_{tn}$  describes the potential, at which the process in the electrolysis cell is neither endothermic nor exothermic; the electrical losses equal the heat required by the endothermic electrolysis process, and describes the total energy demand for the reaction. It can be calculated by equation (1), with  $\Delta H_f$  being the enthalpy of formation of water or steam,  $n$  is the number of electrons involved in the reaction, and  $F$  is Faraday's constant ( $96485 \text{ C}\cdot\text{mol}^{-1}$ ).

$$E_{tn} = \frac{-\Delta H_f}{nF} \quad (1)$$

The thermo-neutral voltage  $E_{tn,0}$  at standard temperature and pressure (STP, 25 °C, 101.325 kPa) is 1.481 V for  $\Delta H_f^0 = -285.840 \text{ kJ mol}^{-1}$ . The enthalpy for water splitting can be calculated using enthalpies from steam tables for temperatures above 25 °C.

$E_{tn}$  as a function of temperature at standard pressure is shown in Figure 19. It must be pointed out that parts of the figure are only theoretical, since water at standard pressure and temperatures above 100°C becomes steam and steam will partly condensate to water below 100 °C, respectively. The theoretical values are therefore given as dashed lines. The influence of the pressure to the thermo-neutral voltage is negligible for most practical applications. The numerical change is only 2.2 mV for a pressure change of 100 bar. It will therefore not be calculated explicitly.

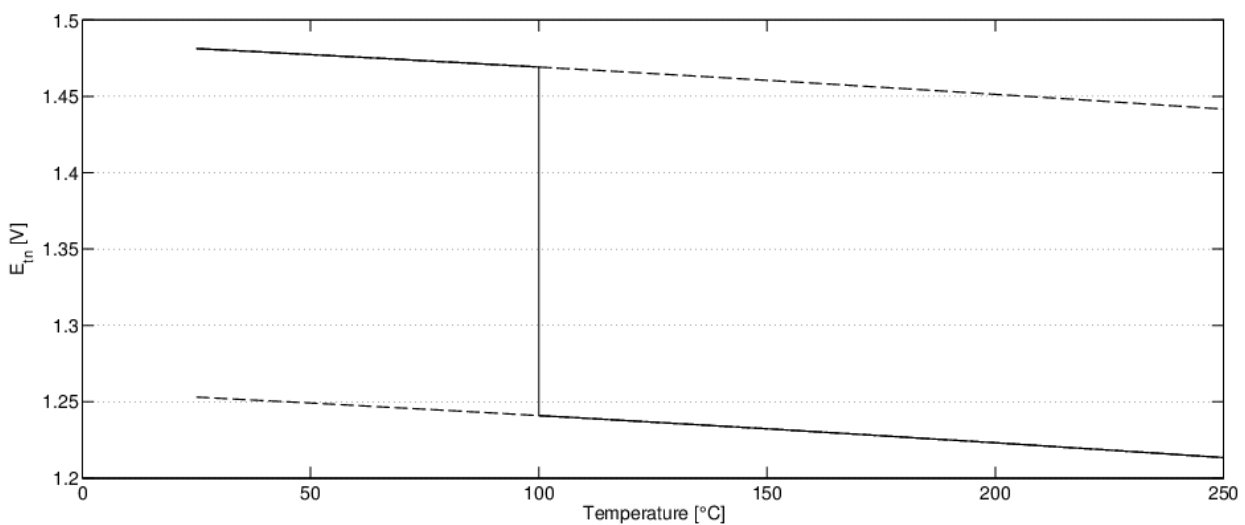


Figure 19. Thermo-neutral voltage  $E_{tn}$  as a function of temperature at standard pressure calculated by empirical equations given by LeRoy et al.

The reversible (or equilibrium) cell voltage,  $E_{rev}$ , is the minimal voltage at which electrolysis of H<sub>2</sub>O is possible and can be calculated by equation (2), where  $\Delta G_f$  is the Gibbs free energy of the reaction,  $n$  is the number of electrons involved in the reaction, and  $F$  is Faraday's constant. At standard conditions it is 1.229 V with  $\Delta G_f^0 = -237.178 \text{ kJ mol}^{-1}$ .

$$E_{rev} = \frac{-\Delta G_f}{nF} \quad (2)$$

A comparison of the electrical energy demand, the total energy demand and the heat demand for water electrolysis at standard pressure is shown in Figure 20 with thermodynamic data obtained from FactSage, a commercial electronic data package and calculation program. It is shown that the electrical energy demand for water electrolysis decreases with increasing temperature, while heat demand rises and the total energy demand is almost constant both for the liquid and the gaseous phase.

As it is not common to perform electrolysis at standard conditions, it is necessary to know both the influence of pressure and temperature to the reversible cell voltage. The reversible cell voltage as a function of temperature and pressure,  $E_{rev(T,p)}$ , can be calculated by equation (3), where  $R$  is the Gas constant ( $8.3144621 \text{ J mol}^{-1} \text{ K}^{-1}$ ),  $a_{H_2}$  is the hydrogen activity,  $a_{O_2}$  is the oxygen activity,  $a_{H_2O}$  is the activity of water and  $T$  is the temperature in Kelvin.

$$E_{rev(T,p)} = \frac{-\Delta G_f}{nF} = \frac{-\Delta G_f^0}{nF} + \frac{RT}{nF} \ln \left( \frac{a_{H_2} a_{O_2}^{\frac{1}{2}}}{a_{H_2O}} \right) \quad (3)$$



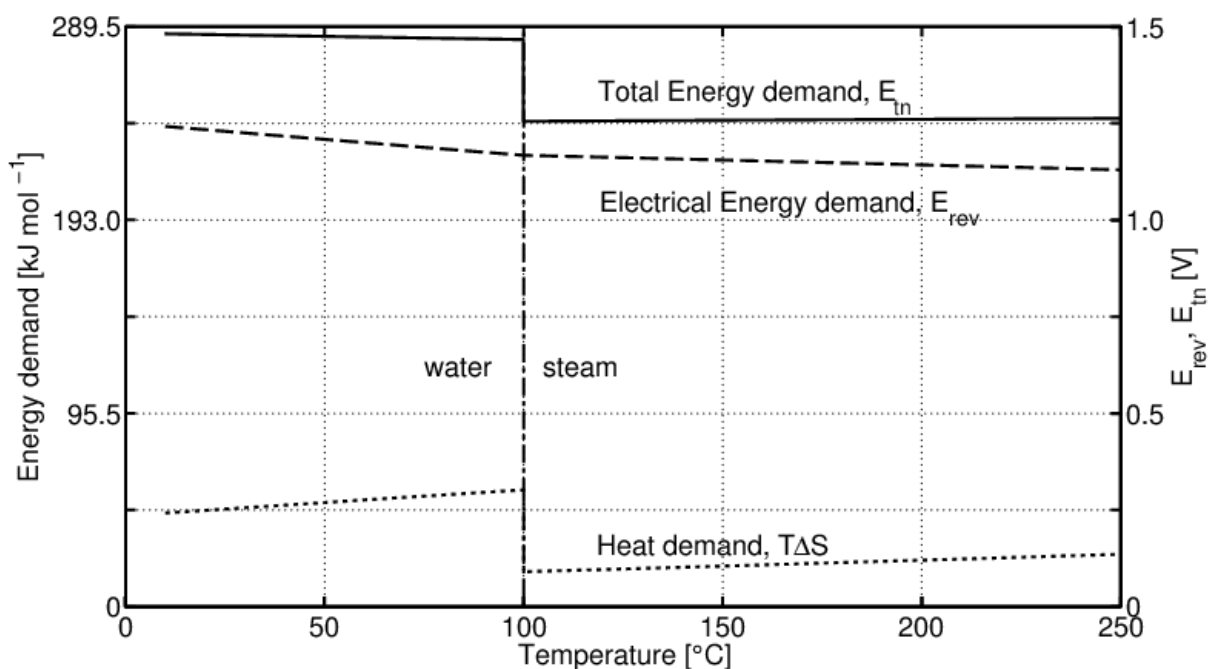


Figure 20 Temperature dependence of the total energy demand,  $\Delta H_f$  (full line), the electrical energy demand,  $\Delta G_f$  (dashed line), and the heat demand  $T \cdot \Delta S_f$  (dotted) for water ( $T \leq 100$  °C) and steam ( $T \geq 100$  °C) electrolysis at 1 bar using data from FactSage.

$E_{rev}(T, p)$  can also be obtained from steam tables or CALPHAD (Computer Coupling of Phase Diagrams and Thermochemistry) programs like FactSage, which include data for  $\Delta G_f$  at elevated temperatures and pressures. Figure 20 reveals that if surplus heat is available to raise steam at the pressure of the electrolyser then a gain in electrical efficiency of several percent is obtained. At 1 bar it amounts to 13 % electrical energy that may be substituted with thermal energy. Furthermore, Figure 20 reveals that an electrolyser operated near above  $E_{tn}$  is self-cooling, i.e. no cooling arrangement is necessary. The cell voltage has to be slightly above  $E_{tn}$  in order to compensate for heat loss to the surroundings. The size of heat loss is naturally dependent on the degree of insulation of the electrolyser.

### ***Solubility of oxygen and hydrogen in aqueous KOH and water***

Tromans developed a formula to predict the oxygen solubility in different inorganic solutions. This formula is said to be feasible to predict the oxygen solubility in potassium hydroxide solutions in a wide range of pressures, temperatures and concentrations. The comparison of his formula with available data showed satisfying accuracy up to 100 °C, but for higher temperatures no data are available.

Figure 21 shows the variation of the oxygen solubility in potassium hydroxide solution as a function of the temperature and different concentrations of KOH (aq). It is seen that the solubility is decreasing strongly with increasing concentration. It is also seen that the solubility has a minimum at around 100 °C. The prediction was shown to be valid for temperatures up to the boiling point of the solution at ambient pressure. Comparison of Tromans formula with data for other solutions that he described in his work, i.e. NaOH, indicates that his formula is accurate and can be used also for temperatures above 100 °C.

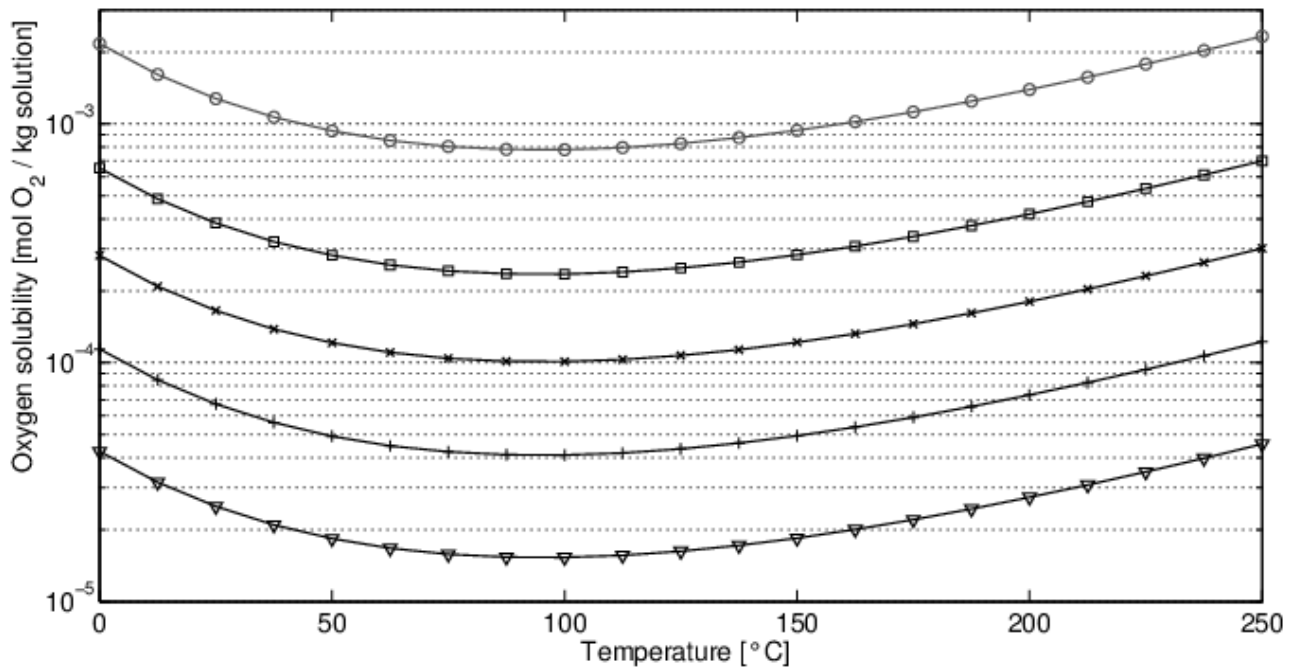


Figure 21 Oxygen solubility as a function of temperature in water (o) and aqueous solutions of KOH for a concentration of 15 wt% (□), 25 wt% (x), 35 wt% (+), and 45 wt% (▽). The solubilities were calculated after an empirical formula developed by Tromans.

Hydrogen seems according to the literature to be in the order of 30 % less soluble than oxygen in aqueous KOH at 30 °C. The pressure dependence of the  $O_2$  and  $H_2$  solubility follows the simple equation (4), where  $c_{i(T, P_i)}$  is the solubility of the species  $i$  as a function of temperature and pressure,  $c_{i(T)}$  is the solubility of the species  $i$  as a function of temperature,  $P_i$  is the partial pressure of the species  $i$  above the solution and  $P_{i, 0}$  is the pressure at which the data were obtained.

$$c_{i(T, P_i)} = c_{i(T)} P_i P_{i, 0}^{-1} \quad (4)$$

Experiments have shown that the solubility of oxygen and hydrogen in aq. KOH as a function of the temperature have minimum around 100 °C, where the solubility is approx. two times lower than at 25 °C. At 250 °C it was shown that the solubility increases to values more or less two times higher than at 25 °C for the  $O_2$  solubility in water and KOH solutions. The  $H_2$  solubility in water is approx. four times higher at 250 °C than at 25 °C. The solubility of oxygen and hydrogen as a function of the KOH concentration decreases strongly with increasing concentration. The  $O_2$  and  $H_2$  solubility in 35 wt% KOH is approx. 21 and 30 times lower, respectively, than that of pure water. Since no experimental solubility data for  $O_2$  and  $H_2$  in KOH (aq) are available above 100 °C, the theoretical values must be taken with care until they are validated experimentally.

### 5.3.3. Constructed measurement set-ups

Three different measurements set-ups were constructed as part of this project. 1) An atmospheric pressure three-electrode set-up in order to get quickly started and to compare results with other project partners. 2) A single atmosphere pressurized set-up and 3) a fully automated set-up with a cell house for test of 4 cells at a time with different (the relevant) atmospheres on each electrode.

#### *Atmospheric pressure three-electrode set-up*

The 1 bar pressure set-up was built in order to study half-cell reactions of electrochemical cells. For this purpose it is common to use a so called 3 electrode setup, which consists generally of a working electrode (WE), a reference electrode (RE) and a counter electrode (CE). The WE is the electrode of interest. It is important to perform measurements under a defined atmosphere; a sufficient amount of gas stream through the electrochemical cell is therefore necessary and can for example be realized as shown schematically in Figure 22: Argon or air can be flushed through a beaker in order to wash and humidify the gas before it enters the electrochemical cell. Furthermore, continuous gas flow ensures that no explosive gas mixtures will occur in the cell beaker from hydrogen and oxygen evolution. The electrical contacts of the WE, RE and CE are connected to a potentiostat in order to perform electrochemical measurements like cyclic voltammetry (CV) or electrochemical impedance spectroscopy (EIS).

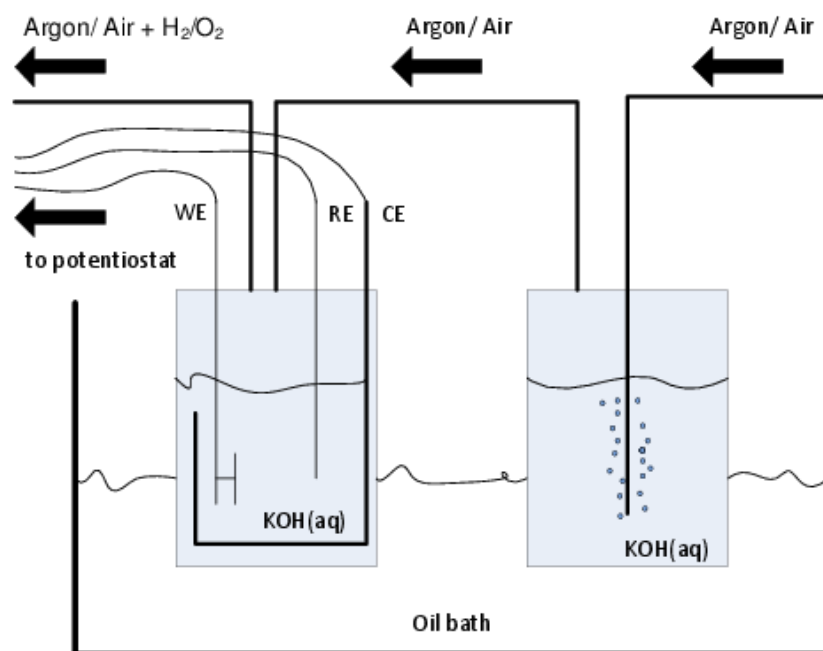


Figure 22 Schematics of the assembly of an atmospheric 3 electrode setup for electrochemical measurements in aqueous solutions. The working electrode (WE), the reference electrode (RE) and the counter electrode (CE) are connected to a potentiostat in order to perform electrochemical measurements. Argon or air can be flushed through a beaker (right beaker) in order to wash and humidify the gas before it enters the electrochemical cell (left beaker). A heated oil bath allows measurements at elevated temperatures

### *Single atmosphere high temperature and pressure set-up*

Next a single atmosphere high temperature and pressure set-up was built. For this purpose it was necessary to build a measurement system around an autoclave which could stand high temperatures up to 250 °C and pressures up to 95 bar as well as extremely caustic environments. PTFE and PFA would be feasible for the high temperatures, but not for the high pressures. A metallic autoclave had to be built or ordered after a careful selection of construction materials. Inconel alloy 600 is recommended for alkalis from Special Metals Corporation, but it is recommended to anneal the alloy if stress corrosion cracking is an issue. Anyway, Inconel 600, also called Alloy 600, showed the most promising resistances among the metals which are available for autoclave construction. After comparing the variety of choices on the market and obtaining quotations from different suppliers, a Parr autoclave Type 4760 was ordered. The technical specifications are listed in Table 3.

Producer	Type	Vessel material	Volume	P <sub>max</sub>	T <sub>max</sub>	Liner	T <sub>max</sub> with liner
Parr Instruments	4760	Inconel 600	600 ml	200 bar	350 °C	PTFE	250 °C

**Table 3** Technical specifications of the Parr autoclave

To perform electrochemical measurements, the autoclave had to be equipped with additional gas handling components and fittings as well as wire feed-throughs. The complete setup is shown in Figure 23; A gas bottle (here shown as nitrogen) is used for the pressurization of the autoclave. A pressure reduction valve PrR1 was installed to avoid too high pressure increase rates and over-pressurization of the system during initial pressurization. The back-flow protection valve BFP1 avoids the back-flow of hazardous gases in the gas bottle. The pressure is adjusted by manually stopping the flow of pressurized gas to the autoclave by needle valve NV1. The J-Type thermo-well T1 measures the Temperature in the autoclave. The pressure gauge PG1 displays the actual pressure analogue in order to allow steady control, even if the electricity supply to the system fails, while another pressure gauge allows recording the pressure together with the temperature in the temperature controller unit. A Teflon liner TL1 protects the inner part of the autoclave from corrosion.

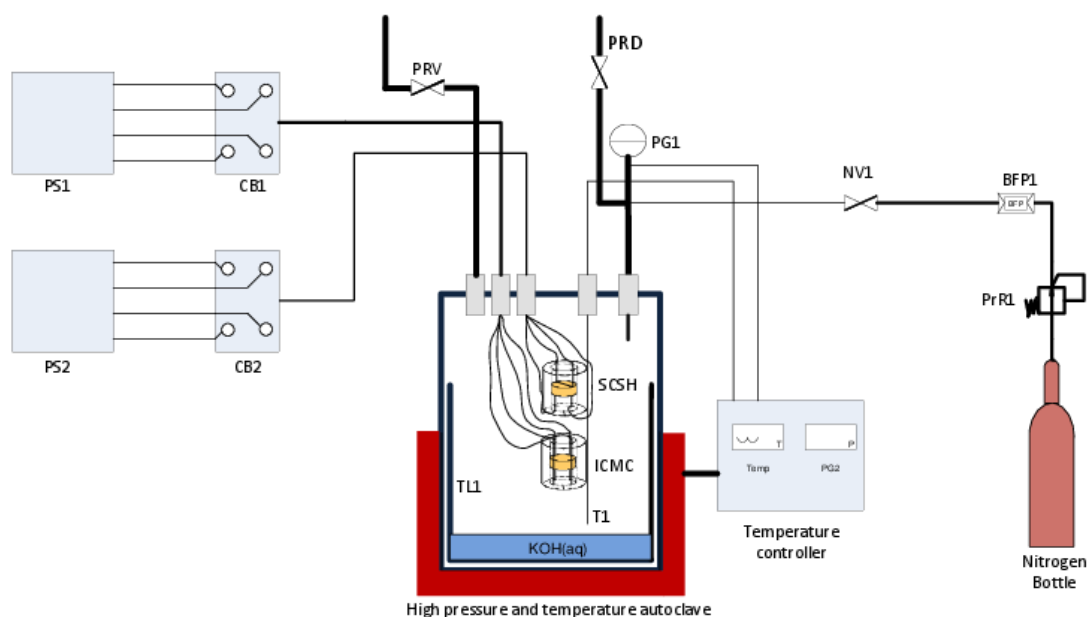


Figure 23 Schematic description of the measurement setup: PrR1= Pressure reducer, BFP1= Backflow protection, NV1= Needle valve, T1= J- Type thermo-well, PG2= Pressure gauge, TL1= Teflon liner, SCMC= Symmetrical Cell Sample Holder, ICMC= Immobilized conductivity measurement cell, CB1& CB2= Connection boxes, PS1 & PS2= Gamry Type 600 potentiostat.

The sample holders, for example the aqueous conductivity measurement cell ACMC, was connected to the protection hood of the thermo-well by a PTFE shrinking tube in the center of the autoclave. The immobilized conductivity measurement cell ICMC was situated directly below and equally fixed. Other sample holders were fixed in a comparable way. The connection wires from each cell were put through to the outside of the autoclave by high pressure glands (the wire feed-throughs) and were then connected to the connection boxes CB1 or CB2. A Gamry Type 600 or 3000 potentiostat, PS1 and PS2, was used to perform the electrochemical measurements. An aqueous solution of potassium hydroxide with lower concentration of than the sample being measured was placed at the bottom of the Teflon liner to avoid drying of the samples during the measurements. Figure 24 shows a sketch of a convenient sample holder used in this setup.

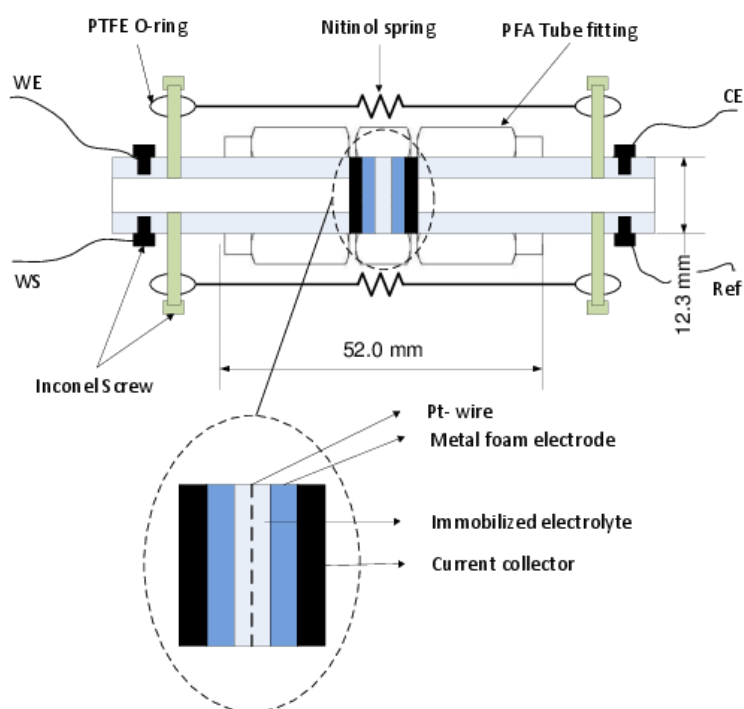


Figure 24 Principal cross section of the Alkaline Electrolysis Cell Holder (AECH): The electrolysis cell is centered in the sample holder. A piece of metal foam acts as current collector. The Inconel tubes press the foam against the active electrode of the electrolysis cell. Nitinol springs are assembled to provide constant force in order to avoid contacting problems. They are insulated against the screws by a PTFE O-ring. The wires WE, WS, CE and Ref indicate how the cell was connected to the potentiostat. The Pt-wire acts as reference electrode in the three electrode setup.

### *Automated high temperature and pressure setup*

The measurements which were performed in the Parr autoclave as described above were time limited to avoid the formation of explosive gas mixtures in the reaction chamber. In order to perform measurements over an extended period of time it was necessary to construct a system which is able to supply the reaction chamber with a continuous flow of  $H_2$ ,  $O_2$ ,  $N_2$  and steam. Since it was desired to have an automated operation of the system at temperatures of up to 300 °C and pressures of up to 95 bar, a number of safety issues had to be considered. The design and construction work were done by specialized employees in order to fulfill the safety demands. The completed two systems with the internal identification names “Rig 28” and “Rig 29” (a similar system in which the Parr autoclave was implemented eventually) are shown in Figure 25 along with the external gas supply panel and the mobile unit for data acquisition.

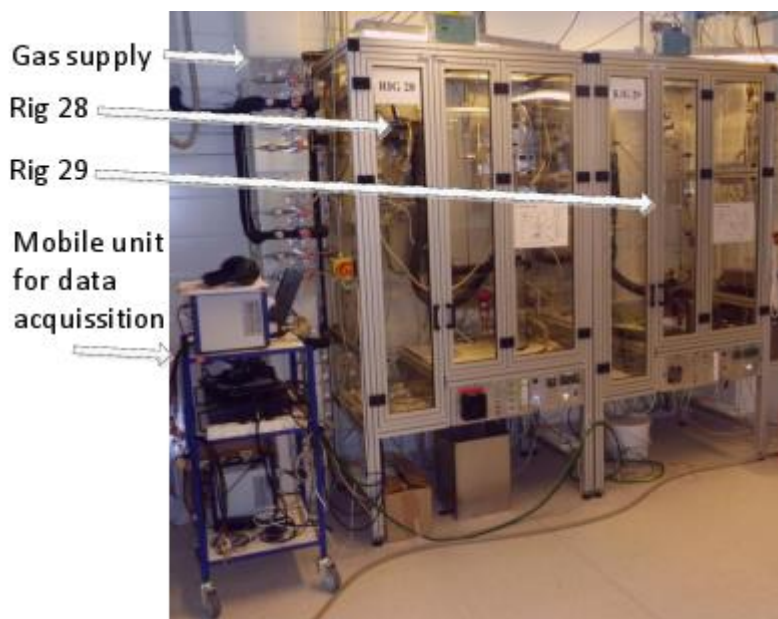


Figure 25 Test rigs 28 and 29 for automated electrochemical tests in the temperature range from room temperature to 250 °C and pressures up to 95 bar. The mobile unit for data acquisition consists of two Gamry type 3000 potentiostats, a 8 channel multiplexer and a personal laptop computer.

A detailed diagram comprising the used actuators is shown in Figure 26. The gases enter the autoclave through the inlets 3, 5 and 7 in Figure 26.  $N_2$ ,  $CO_2$  and  $O_2$  are fed through one tube (inlet 3) and  $H_2$  is fed through inlet 7 to the catalytic burner (CB). The CB comprises a honeycomb structured ceramic body with a catalyst to allow steam generation by  $H_2$  and  $O_2$  combustion in the autoclave with a known flow rate, controlled by mass flow controllers. An excess of  $H_2$  or  $O_2$  can be programmed for the case that measurements should be performed in reducing or oxidizing atmosphere. A second catalytic burner placed right below the cell holder and before the outlet of the autoclave, ensures that the  $H_2$  and  $O_2$  produced by electrolysis will recombine into  $H_2O$  before exiting the autoclave. (The shown mass spectrometer (MS) and the heated  $CO_2$  and transfer lines are used for other projects that have contributed to the construction of these rigs).

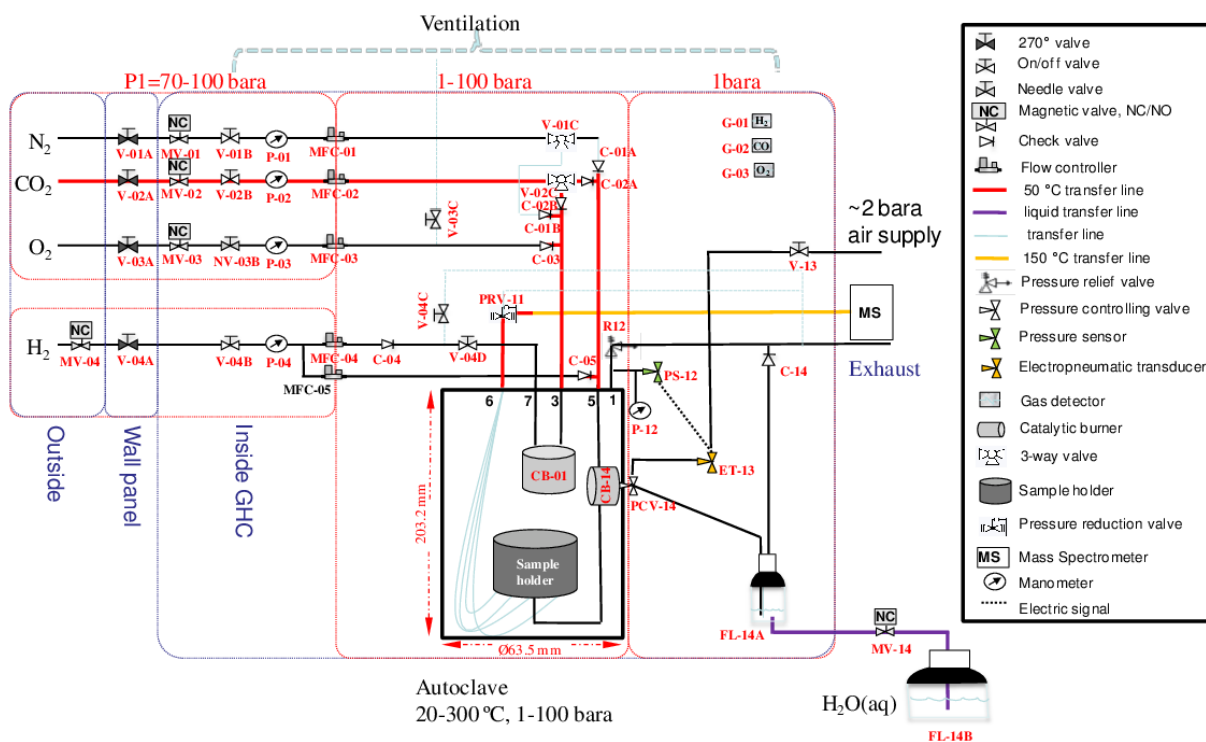


Figure 26 Rig 28 gas handling system

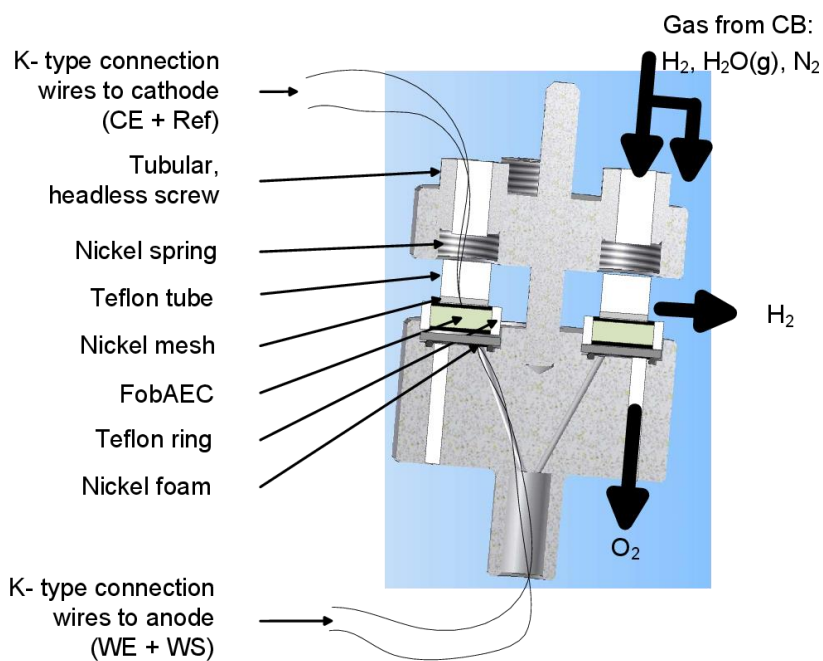


Figure 27 Illustration of the sample holder used in the autoclave to test the electrolysis cells with mounted sample and simplified demonstration of the gas flow. FobAEC is the abbreviation used for (metal) foam based alkaline electrolysis cell.



The sample holder used to test the produced electrolysis cells is schematically shown in Figure 27. A K-type thermocouple is used to connect the cathode of the metal foam based alkaline electrolysis cell, FobAEC, to the counter electrode (CE) and reference input (Ref) of the potentiostat multiplexer. A tubular, headless screw is used to fix the setup initially. A nickel spring ensures that the nickel mesh, which is wrapped around a Teflon tube, is pressed to the cathode during the measurements. A Teflon ring has been placed around the FobAEC to avoid gas mixing. A layer of nickel foam is used as current collector at the anodic side of the FobAEC. Another K-type thermocouple is connected to the nickel foam current collector on the sample bottom. It is connected to the working electrode (WE) and the working sense (WS) of the potentiostat. The same connections were used on the right sample shown in Figure 27, but have not been drawn for clarity reasons.

The gas mixture from the catalytic burner CB at the gas inlet (in the experiments discussed later on a mixture of  $H_2$ ,  $H_2O$  and  $N_2$ ) flows partly to the cathode of the FobAEC and further through the autoclave. The oxygen produced at the anode of the FobAEC escapes the sample holder through a tubular hole, where it will mix with the other gases and react to form steam at the CB placed at the autoclave outlet. A pressure control valve is placed at the outlet stream of the autoclave to set the gas pressure to the desired value.

#### 5.3.4. Specific electrical conductivity measurements on free and immobilized aqueous KOH

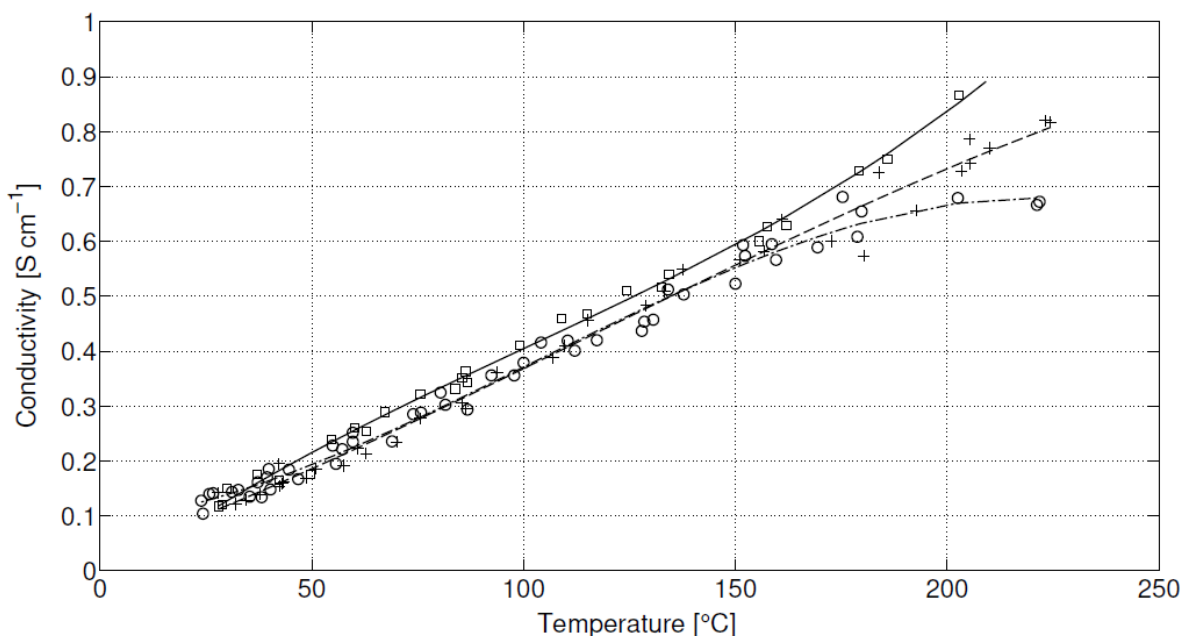


Figure 28 Measured conductivity and cubic regression analysis for 35 wt% (o = measured, dash-dotted line = regression), 45 wt% (□ = measured, full line = regression) and 55 wt% (+ = measured, dashed line = regression) immobilized KOH (aq) as a function of temperature and a pressure of 25-40 bar.

The conductivity of aqueous KOH at elevated temperatures and high concentrations was investigated using the van der Pauw method in combination with electrochemical impedance spectroscopy (EIS). Conductivity values of  $2.7 \text{ S cm}^{-1}$  for 35 wt%,  $2.9 \text{ S cm}^{-1}$  for 45 wt%, and  $2.8 \text{ S cm}^{-1}$  for 55 wt% concentrated aqueous solutions were measured at  $200 \text{ }^\circ\text{C}$ . Micro- and nano-porous solid  $\text{SrTiO}_3$  pellets were produced and used to immobilize aqueous KOH solutions. These are intended to operate as the ion-conductive electrolytes in alkaline electrolysis cells, offering high conductivity and corrosion resistance. The conductivity of immobilized KOH has been determined by the same method in the same temperature and concentration range. Conductivity values as high as  $0.67 \text{ S cm}^{-1}$  for 35 wt%,  $0.84 \text{ S cm}^{-1}$  for 45 wt%, and  $0.73 \text{ S cm}^{-1}$  for 55 wt% concentrated immobilized aqueous solutions were determined at  $200 \text{ }^\circ\text{C}$ . Furthermore, phase transition lines between the aqueous and aqueous + gaseous phase fields of the KOH/ $\text{H}_2\text{O}$  system were calculated as a function of temperature, concentration and pressure in the temperature range of  $100\text{-}350 \text{ }^\circ\text{C}$ , for concentrations of  $0\text{-}60 \text{ wt}\%$  and at pressures between 1 and 100 bar. Figure 28 gives the data for the immobilized electrolytes.

### 5.3.5. Alkaline electrolysis cell for $250 \text{ }^\circ\text{C}$ and 40 bar

A new type alkaline electrolysis cell and method to produce them has been developed based on inspiration from literature and a long “trial and error” process. We call it metal foam based alkaline electrolysis cell, FobAEC, even though several variants of the cell type have been produced and tested as described in this section.

#### *Principle of metal foam based alkaline electrolysis cell with immobilized KOH*

A porous structure in which the liquid electrolyte is immobilized by capillary forces can be used as a combination of diaphragm and electrolyte. In this case, the reduced free volume for the liquid electrolyte and the tortuosity of the porous structure are expected to result in a decrease in conductivity, and by that to an increase in ohmic losses. Nevertheless, the ohmic losses can be reduced by reducing the thickness of the porous structure. A great advantage of immobilizing the electrolyte is the possibility to use gas diffusion electrodes (GDEs) for steam electrolysis at temperatures well above the boiling point of water, i.e. up to  $250 \text{ }^\circ\text{C}$  in case of pressurization, while the electrolyte remains in the liquid phase. At any given temperature, it is important to operate within an appropriate pressure range since too high pressures could cause condensation of steam (and thereby dilute the electrolyte and/or flood the GDE) while too low pressures could cause evaporation of the electrolyte (through which ohmic losses would increase).

Gas diffusion electrodes allow in principle electrolysis without the formation of gas bubbles, which usually leads to increased ohmic losses due to area reduction and increased anodic and cathodic overpotentials due to reduced available electrode area. GDEs have to be highly electronic conductive to minimize ohmic losses, and porous to allow the produced gases to escape while steam flows into the cell towards the triple phase boundary, TPB, as shown in Figure 29, which illustrates the FobAEC. Since the electrochemical reactions take place at or near the TPB only, it is important that the TPB-length is as long as possible. Nickel is known to be corrosion resistant in alkaline media and electro-catalytically active, hence it is often used as a base material for electrodes in alkaline electrolysis cells. Electro-catalysts are optimally placed at the TPB in order to achieve low overpotentials. Silver is known to be an excellent catalyst for the oxygen reduction

reaction, ORR, in alkaline fuel cells and can be considered as catalyst for the oxygen evolution reaction, OER, as well.  $\text{Co}_3\text{O}_4$  and Co-based spinel oxides are also known to be good electro-catalysts for the OER, and Raney-nickel and molybdenum are preferred electro-catalysts for the hydrogen evolution reaction, HER. The anodic overpotential caused by the OER is usually dominating over the cathodic overpotential caused by the HER.

Nickel foams are widely used and have already been shown to work as a gas diffusion electrode for the ORR in an alkaline fuel cell. More advanced metal foams have recently been developed from Alantum Europe GmbH, where metal alloy foams are obtained by a powder metallurgical process. Important material parameters, i.e. final composition, the specific surface area, and the pore size of the foam can be customized to the application.

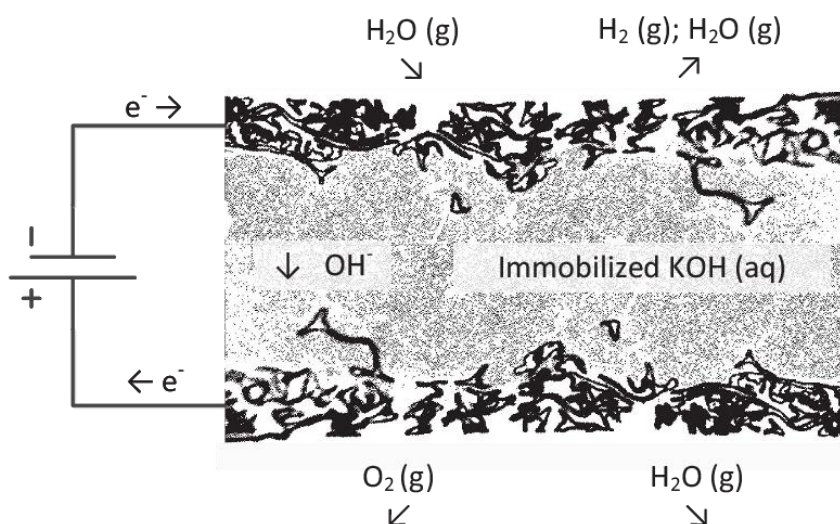


Figure 29 Illustration of an alkaline electrolysis cell with KOH (aq) electrolyte immobilized in a porous matrix and gas diffusion electrodes.

The foam based alkaline electrochemical cells (FobAEC) were produced from metal foams delivered by Alantum Europe GmbH. Circular foam pieces with a diameter of 12 mm were stamped out of the foam sheets with a thickness of 1.0 mm for nickel foam, and 1.6 mm for Inconel 625 foam (Inconel 625 alloy composition is for example in wt%: Cr, 21.32; Mo, 8.58; Nb, 3.73; Al, 0.18; Ti, 0.16; Fe, 0.11; Si, 0.09; C, 0.053; Mn, 0.04; Mg, 0.01; Balance Ni). The circular foam pieces were cleaned in ethanol; beside that, the foams were used as delivered. One or two foam layers are placed in a uni-axial press and 0.25-1.5 g  $\text{SrTiO}_3$  powder is placed on top of the foam. One drop of an appropriate binder, i.e. MEK in 33 % ethanol, has been mixed to 100 mg of the perovskite  $\text{SrTiO}_3$  powder to obtain better adhesion of the powder particles during processing and sintering. Another one or two layers of foam is placed on top of the powder. The whole structure is pressed for 30 s with a pressure of  $13.0 \text{ kN cm}^{-2}$ . The cells have then been sintered in air at  $450 \text{ }^\circ\text{C}$  for 2 h with a heating ramp of  $100 \text{ K h}^{-1}$  followed by a second sintering step in 9 %  $\text{H}_2$  in Ar at  $1000 \text{ }^\circ\text{C}$  for 6 h with a heating and cooling ramp of  $50 \text{ K h}^{-1}$ .

Electrodeposition of silver was performed onto some of the cells in order to improve the performance of the anode for the OER. The electrodeposition was performed with a 0.1 M AgNO<sub>3</sub> + 1 M KNO<sub>3</sub> solution under N<sub>2</sub> atmosphere and stirring. Pulsed deposition with pulse/pause relation of 1s/1s and a potential difference of -3.0 V (vs. a platinised Pt counter electrode) has been used to deposit the Ag particles on the foam with a Gamry type 600 or 3000 potentiostat. Scanning electron microscopy SEM was used to analyse the surface and cross section of the FobAEC before and after measurements. SEM (Scanning electron microscopy) images of the untreated foam are shown in Figure 30. The pore size of the nickel and Inconel foam is ca. 450 μm with a porosity of 95 % for the nickel foam and > 91 % for the Inconel foam according to the manufacturers' specification. It can be seen that the surface of the nickel foam is relatively smooth compared to this of the Inconel foam. The coarse layer on the Inconel foam shows the Inconel layer, which has been coated on nickel foam (left part of Figure 30).

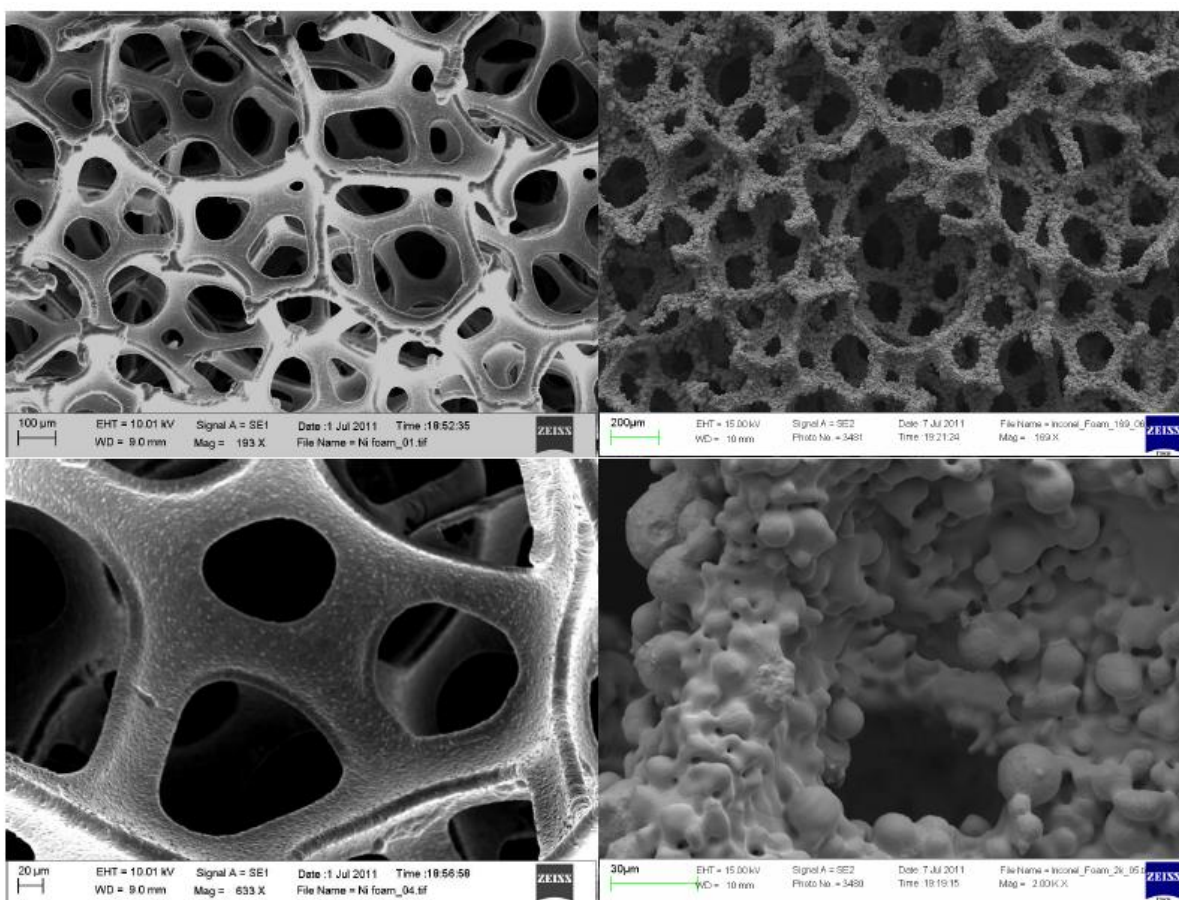


Figure 30 SEM picture of untreated nickel foam (upper-left and lower-left) and Inconel foam (upper-right and lower-right). Note: the magnifications are different as indicated by the scale bars.

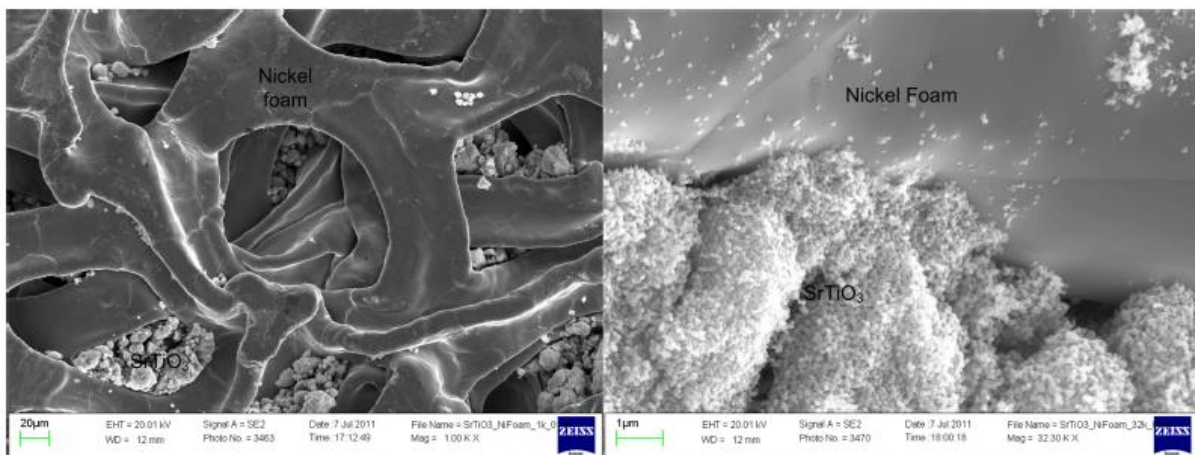


Figure 31 SEM picture of the surface of the nickel foam anode of a FobAEC at low (left), and high magnification (see scale bar) showing the interface between the nickel foam and the SrTiO<sub>3</sub> (right).

The porosity of the foam is significantly reduced after pressing of the whole cell body in the uni-axial press. The typical pore size diameter is reduced to values in the order of  $150 \mu\text{m} \pm 50 \mu\text{m}$  with an even distribution. The shape is naturally changed to a more flat form instead of being ball-like, as it can be seen in Figure 31, left image. The highly porous SrTiO<sub>3</sub> structure sticks out of the nickel foam at several places up to the surface of the cell. It can be seen that the nickel foam can act as a current collector as well as the active electrode in such structure. The right image of Figure 31 shows the interface of the SrTiO<sub>3</sub> and the nickel foam, which will act as the TPB after immersion of the cell into liquid electrolyte. The SrTiO<sub>3</sub> has a tendency to form clusters on the surface which have a size of ca.  $2 - 10 \mu\text{m}$ , while the pore size is mainly distributed around 60 nm.

Silver electro-deposition was successfully applied to the nickel foam anode as shown in Figure 32. The left image shows the foam with silver crystals of a particle size in the region of  $10 - 20 \mu\text{m}$  and nano sized silver particles distributed all over the foams surface. The right image shows the interface of the same sample at higher magnification where a relatively large silver particle of  $7.5 \mu\text{m}$  can be seen in the upper left part with well distributed nano sized particles in the range of  $50 - 500 \text{ nm}$ .



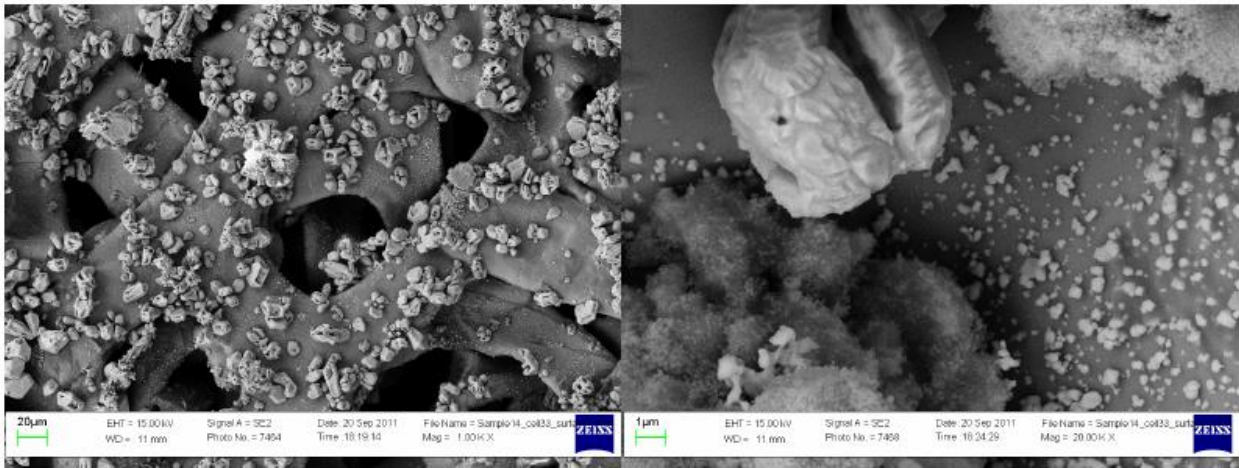


Figure 32 SEM picture of the surface of the nickel foam after Ag electrodeposition of the anode of a FobAEC at low (left) and high magnification (see scale bar) (right) showing the interface between the nickel foam and SrTiO<sub>3</sub> as well as the nano sized Ag particles

The results of the cross section analysis are shown in Figure 33. The brightest structure indicates the metal foams, light grey is the porous SrTiO<sub>3</sub> structure and dark grey is the surrounding epoxy coating for the SEM analysis. Both electrodes are pressed out of two layers of the corresponding metal foam. The Inconel foam is less compressed than the nickel foam and shows a higher specific surface area than the pure nickel. It can also be seen that it will be sufficient to use only one layer of Inconel foam, but 2 layers of nickel foam are needed in order to obtain a good distribution of gas channels in combination with the ability of the foam to work as a current collector and active electrode.

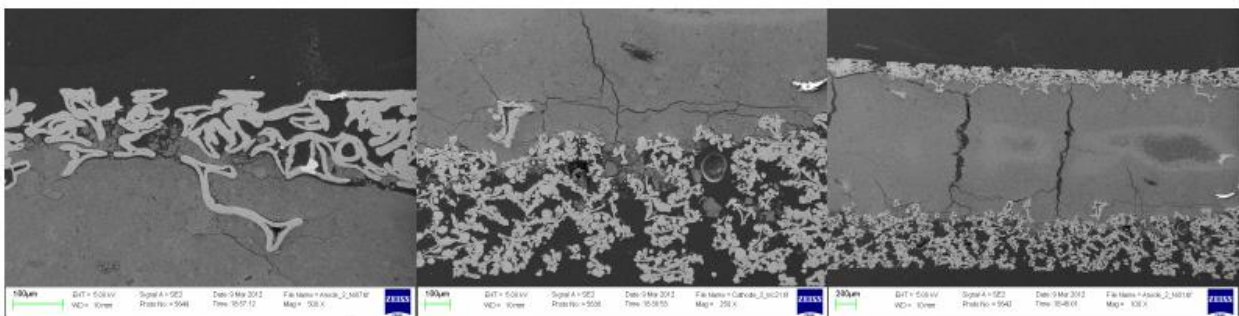


Figure 33 SEM picture of the cross section of a FobAEC with two layers of nickel and two layers of Inconel foam showing the nickel anode (left), the Inconel cathode (center) and the full cell (right).

### Electrochemical performance

The electrochemical testing comprised the 1 bar test of plain Ni and Raney-nickel electrodes for comparison of measurement techniques between the project partners and for creating a kind of reference against which the high pressure and temperature tests could be evaluated. Testing of the FobAEC cell type with different electrocatalysts was carried out in the next step.

### Raney-nickel electrodes at different temperatures

A Raney-nickel sample delivered by FORCE-Technology was tested in the above described atmospheric measurement setup. After activation in 30 wt% KOH with 10% KNa-tartrate tetrahydrate at 80 °C for 24 hrs (Step1), the sample has been conditioned at  $-10 \text{ mA cm}^{-2}$  for 2 hours (Step 2) and at  $-200 \text{ mA cm}^{-2}$  for 14 hours (Step 3) in 25 wt% KOH (aq.) after instructions from FORCE Technology.

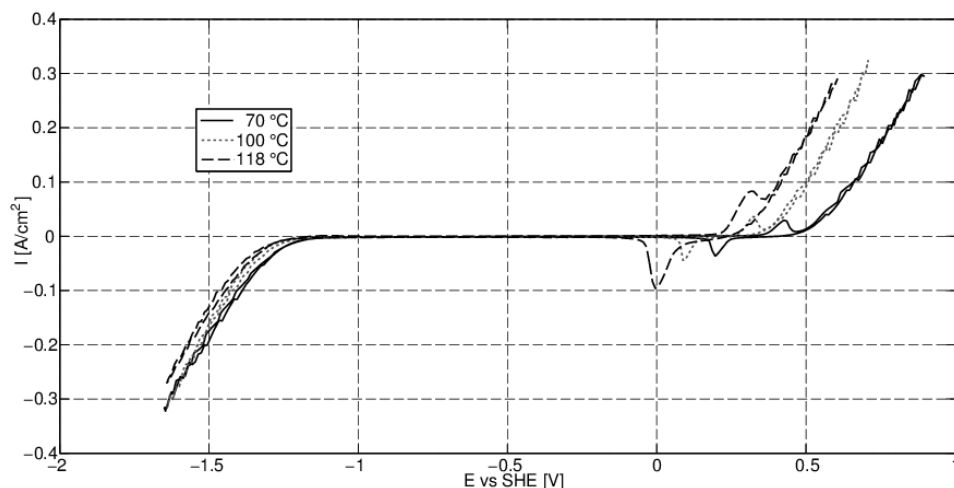


**Figure 34** Cyclic Voltammograms of the Force Raney Nickel electrode under  $\text{N}_2$  atmosphere at ambient pressure and temperatures from 70 °C to 118 °C in 10 M KOH (aq) measured with a sweep rate of  $10 \text{ mV s}^{-1}$ .

Cyclic voltammetry was applied to the activated and conditioned electrode at temperatures of 70 °C, 100 °C and 118 °C. The obtained results are shown in Figure 34. The potential for the OER at a current density of  $200 \text{ mA cm}^{-2}$  was found to be 0.77 V, 0.6 V and 0.51 V for temperatures of 70 °C, 100 °C and 118 °C, respectively. Hence, the anodic polarization was reduced by 260 mV through heating from 70 °C to 118 °C. The potential for the HER at a current density of  $-200 \text{ mA cm}^{-2}$  was found to be -1.52 V, -1.54 V and -1.58 V for temperatures of 70 °C, 100 °C and 118 °C, respectively. All measurements were carried out without IR-compensation.

### Test of FobAEC at high pressure and temperature

Cell performance tests have mainly been performed at temperatures in the region of 250 °C and pressures around 40 bar. Cyclic voltammograms of different compositions of the FobAECs are shown in Figure 35. The current density at a polarization of  $U_{\text{cell}} = 1.5 \text{ V}$  (uncompensated for ohmic resistance) reached from  $466 \text{ mA cm}^{-2}$  at 240 °C and 38 bar (for a cell with 2 layers of nickel foam as anode and two layers of Inconel foam as cathode), to  $1000 \text{ mA cm}^{-2}$  at 240 °C and 37 bar (for a cell with 1 layer of nickel foam with Ag- deposition as anode and one layer of Inconel 625 foam as cathode).

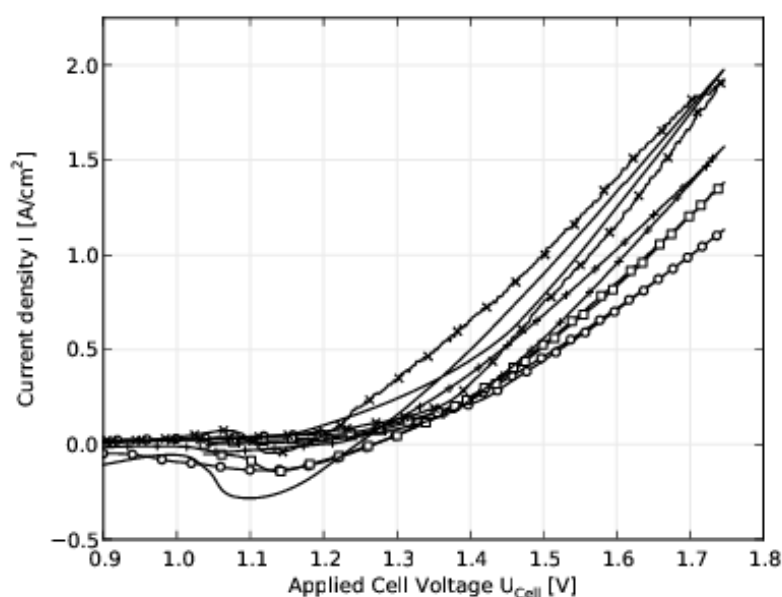


Figure 35 IV- curves of different cells at temperatures around 240 °C and pressures around 40 bar, i.e.: Cell 3a (x) and Cell 3b (full line) with 1 layer Ag- deposited nickel anode and 1 layer Inconel as cathode; Cell 2 (+) with 1 layer nickel foam anode and 1 layer Inconel as cathode; Cell 1b (□) with 2 layers nickel foam anode and 2 layers Inconel as cathode; Cell 1a (o) with 2 layers nickel foam anode and 2 layers Inconel as cathode.

Additional performance data for further cell compositions are shown in Table 4. The serial resistance  $R_s$  has been measured with EIS under polarization of 1.4 V. The Ag- activated cells have shown the best performance as shown in Table 4.

Impedance analysis have generally been performed at a polarization voltage of 1.4 V. Figure 36 shows the cyclic voltammogram for a Ag- activated cell along with polarized impedance measurements before and after recording the voltammogram at polarization voltages of 1.4 V and 1.5 V. The serial resistance  $R_s$  decreased slightly after recording the voltammogram from 133  $m\Omega\text{ cm}^2$  to 125  $m\Omega\text{ cm}^2$  at 1.4 V polarization, while the area specific resistance of the cell,  $ASR_{cell}$ , decreased from 335  $m\Omega\text{ cm}^2$  before, to 319  $m\Omega\text{ cm}^2$  after recording the voltammogram. The  $R_s$  at 1.5 V was equal to this at 1.4 V (125  $m\Omega\text{ cm}^2$ ), whereas the  $ASR_{cell}$  reduced to 250  $m\Omega\text{ cm}^2$ . The main change is associated with the low frequency part of the spectrum indicating an increased gas transport resistance with time.

Cell	Anode	Cathode	Temperature [°C]/Pressure [bar]	$I$ [ $\text{mA cm}^{-2}$ ] at 1.5 V (uncomp.)	$I$ [ $\text{mA cm}^{-2}$ ] at 1.75 V (uncomp.)	$R_s$ [ $\text{m}\Omega\text{ cm}^2$ ] at 1.4 V polarization	$U_{cell}$ [V] at 0.5 $\text{A cm}^{-2}$ (comp.)
Cell 1a	2 layer Ni foam	2 layer Inc foam	240/38	466	1130	148	1.441



Cell 1b	2 layer Ni foam	2 layer Inc foam	237/36	528	1378	140	1.419
Cell 2	1 layer Ni foam	1 layer Inc foam	240/39	679	1570	112	1.388
Cell 3a	1 layer Ni foam + Ag deposition	1 layer Inc foam	240/37	1000	1918	119	1.291
Cell 3b	1 layer Ni foam + Ag deposition	1 layer Inc foam	247/42	903	1978	124	1.337

Table 4 Comparison of the cell performance for different compositions of the FobAEC at around 240 °C and 40 bar.

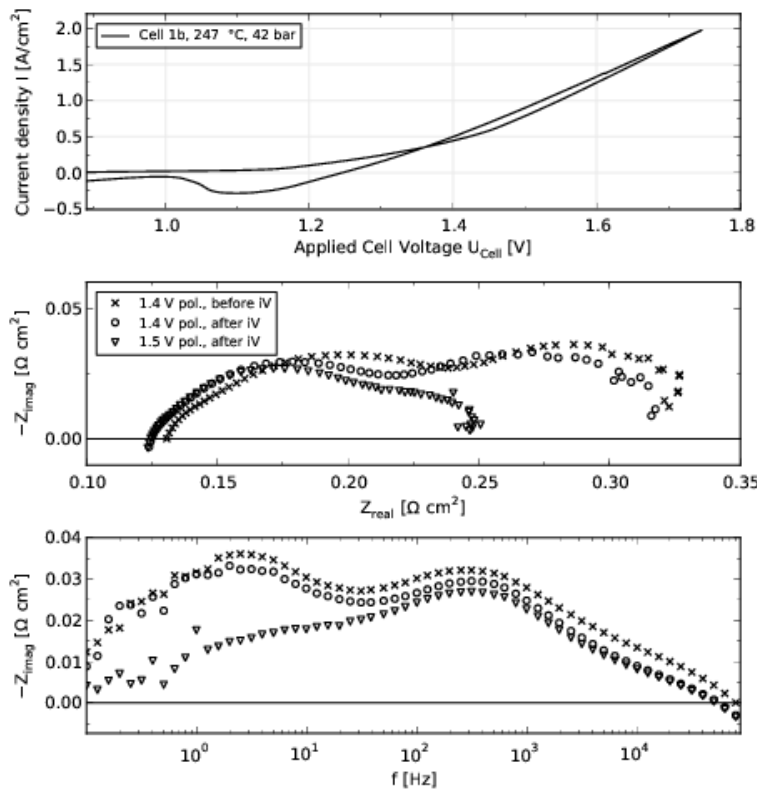


Figure 36 Cyclic voltammogram (upper figure) of a FobAEC with Ag- deposited anode and Inconel cathode at 247 °C and 43 bar in comparison with the corresponding impedance analysis (central figure) at polarization voltages of 1.4 V before (x) and 1.4 V (o) and 1.5 V (∇) after the cyclic voltammetry test.

The performance of a FobAEC with Ag- deposited anode and Inconel cathode at 240 °C and 37 bar, 202 °C and 27 bar and 108 °C and 15 bar in comparison with the corresponding impedance measurements can be seen in Figure 37. The investigated cell showed current densities of 1000 mA cm<sup>-2</sup> at 240 °C, 640 mA cm<sup>-2</sup> at 202 °C and 85 mA cm<sup>-2</sup> at 108 °C at a cell voltage of 1.5 V (during decreasing the cell voltage). The current densities at 1.75 V were 200 mA cm<sup>-2</sup>, 1440 mA cm<sup>-2</sup> and 1940 mA cm<sup>-2</sup> at temperatures of 108 °C, 202 °C and 240 °C, respectively. The results are not R<sub>s</sub>-compensated. The impedance plots at a polarization voltage of 1.4 V show that R<sub>s</sub> improved from 164 mΩ cm<sup>2</sup> to 128 mΩ cm<sup>2</sup>. ASR<sub>cell</sub> improved more significantly from 508 mΩ cm<sup>2</sup> to 361 mΩ cm<sup>2</sup> with increasing temperature from 202 °C to 240 °C as shown in the lower part of Figure 37. The impedance curve shows significant scattering at low frequencies; a Kramers-Kronig test showed an error above 1 % (up to ± 4.5 %) at frequencies below 10 Hz with random distribution around zero.

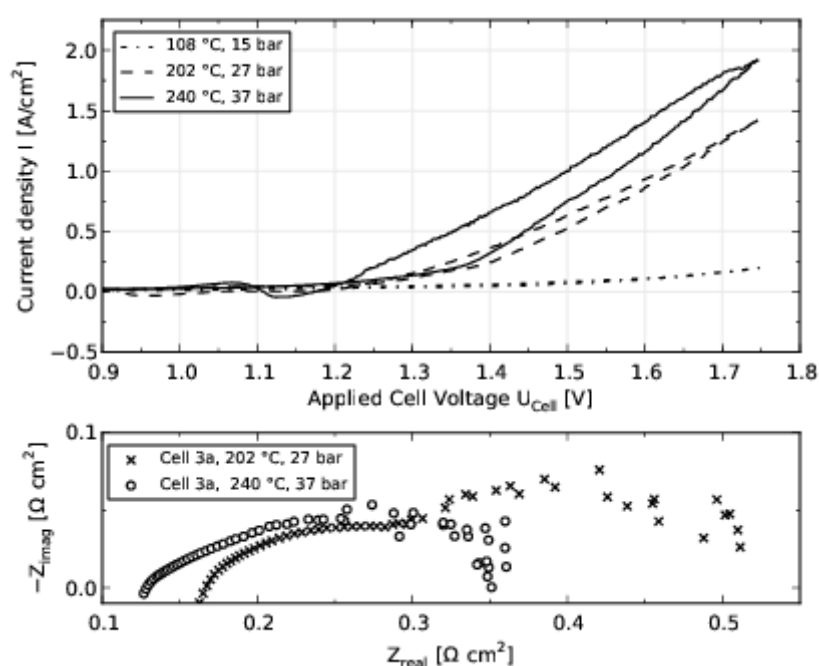


Figure 37 Cyclic voltammogram (upper figure) of a FobAEC (Cell 3a) with Ag- deposited anode and Inconel cathode at 240 °C and 37 bar (full line), 202 °C and 27 bar (dashed line) and 108 °C and 15 bar (dash-dot) along with the corresponding impedance analysis (lower figure) from data achieved at a polarization of 1.4 V.

#### Determination of the hydrogen and oxygen evolution overpotentials

The overpotential of the Inconel cathode has been studied with the use of the sample holder as shown in Figure 24. The reference terminal of the potentiostat was connected to the Pt- wire in the center of the FobAEC, see Figure 24. The Pt-wire acts as a reference electrode. The analysis of the hydrogen evolution reaction, HER, has been performed in safety gas (9 % H<sub>2</sub> in N<sub>2</sub>) with the results for the cyclic sweep voltammogram shown in Figure 38. At a current density of 100 mA cm<sup>-2</sup> the overpotential was - 40 mV and at 1000 mA cm<sup>-2</sup> it was - 131 mV, resulting in a Tafel-slope of 91 mV / dec. The overpotential uncompensated for IR drop at a current density of 1 A cm<sup>-2</sup> was -0.28 V.

The IR- corrected results ( $\eta_{H_2}$ ) correspond to the difference of the cathode potential vs the equilibrium potential of the reference electrode  $E_{eqC}$ . The cathode potential vs the SHE ( $E_{C,SHE}$ ) is displayed on the second ordinate of Figure 38.

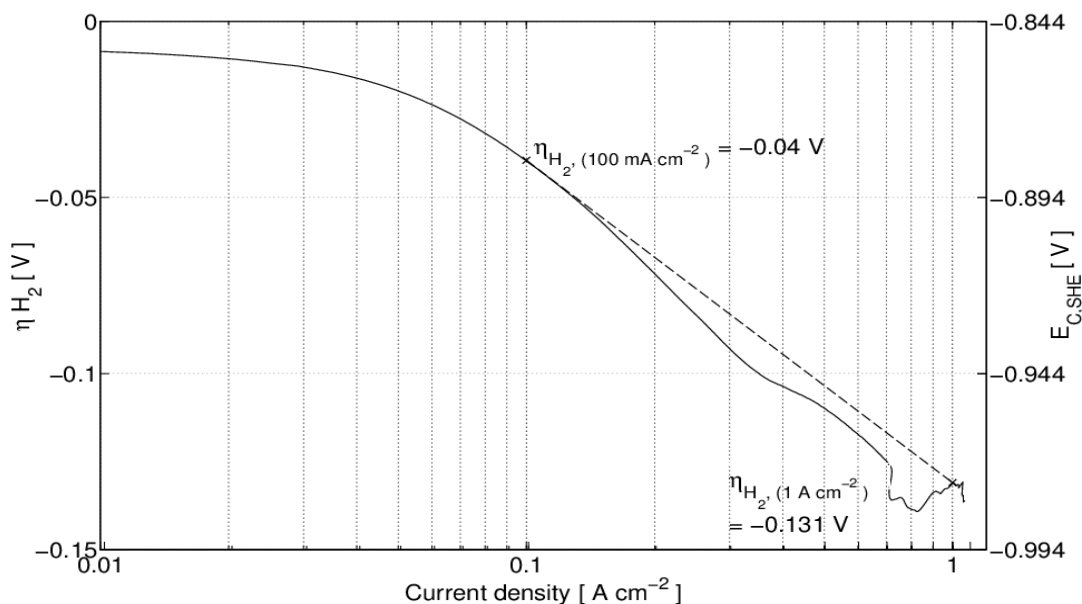


Figure 38 Cyclic voltammogram for the hydrogen evolution overpotential of the Inconel cathode with a sweep rate of 20 mV/s at 42.1 bar and 248 °C. The full line shows the  $R_s$ - compensated applied cell voltage; the dashed line shows the graphical estimation of an Tafel line between  $100 \text{ mA cm}^{-2}$  and  $1 \text{ A cm}^{-2}$ .

The oxygen overpotential has been measured in technical air (20 %  $O_2$ , 80 %  $N_2$ ) for cells with and without the Ag catalyst with the results shown in Figure 39. The obtained current density for low overpotentials between 50 mV and 150 mV is higher for the cell without Ag, but this was not generally the case (compare Figure 35). At higher overpotentials the situation changes and the current density of the Ag activated anode is higher than that of the pure nickel foam anode, i.e. at a current density of  $90 \text{ mA cm}^{-2}$  the overpotentials are 250 mV and 220 mV, while at  $900 \text{ mA cm}^{-2}$  they are 360 mV and 380 mV for the Ag activated anode and the nickel anode, respectively. The Tafel slope for the not activated cell is 160 mV / decade, while the Ag- activated anode improved to 130 mV / decade between  $90 \text{ mA cm}^{-2}$  and  $900 \text{ mA cm}^{-2}$ . The curves appear to be highly nonlinear.

The IR- corrected results ( $\eta_{O_2}$ ) correspond to the difference of the cathode potential vs the equilibrium potential of the reference electrode  $E_{eqA}$ . The anode potential vs the SHE ( $E_{A,SHE}$ ) is displayed on the second ordinate of Figure 39.

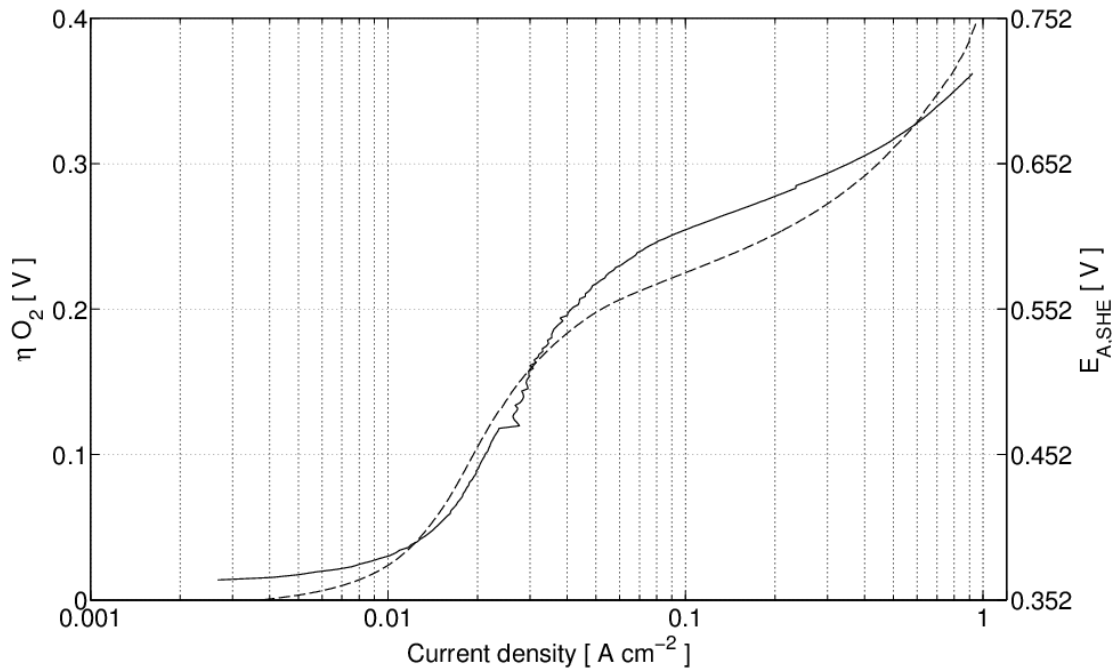


Figure 39 IV-curve of a Ag loaded anode at 43.3 bar and 248 °C (full line) in comparison with an IV-curve of a pure nickel foam anode (dashed) at 42 bar 250 °C, both recorded with a sweep rate of 50 mV/s and compensated for  $R_s$ .

### 5.3.6. “Long term” galvanostatic test

The galvanostatic measurement on cell called cell 70 showed an activation period at the beginning of the measurement.  $U_{\text{cell}}$  at  $t_{\text{el}} = 0$  h was 1.49 V, decreasing to 1.44 V at  $t_{\text{el}} = 5$  h, resulting in an activation rate of 10 mV/h for the first 5 h. With ongoing electrolysis time, cell voltage peaks (irregular oscillations) occurred. The minimum and the maximum value of these peaks are shown in Figure 40 along with the average cell voltage  $U_{\text{cell, mean}}$  for each 5 h lasting measurement period. It can be seen that a relatively strong degradation takes place from  $t_{\text{el}} = 5$  h until  $t_{\text{el}} = 45$  h, with  $U_{\text{cell, mean}}$  starting from 1.45 V and ending at 1.66 V. The resulting degradation rate in this period is 5.25 mV/h. From  $t_{\text{el}} = 45$  h until  $t_{\text{el}} = 230$  h the degradation rate decreased to 0.6 mV/h, ending at  $U_{\text{cell, mean}} = 1.77$  V. Further on, the cell activated again to  $U_{\text{cell, mean}} = 1.67$  V at  $t_{\text{el}} = 345$  h with an activation rate of 0.9 mV/h.

Such an initial activation followed by a degradation process was also observed by Divisek et al. for an electrolysis cell under galvanostatic conditions (400 mA cm<sup>-2</sup>, 100 °C, 10 M KOH); corrosion problems were indicated as the reason for degradation in their measurements. Although viewed in terms of  $U_{\text{cell, mean}}$  cell 70 seems to have activated during that last period, the observed cell voltage peak maximum and repeating rate increased during this time. The galvanostatic impedance measurements which were performed at the end of each 5 h interval led to too high cell voltages for the potentiostat and the measurement was stopped after 350 h.

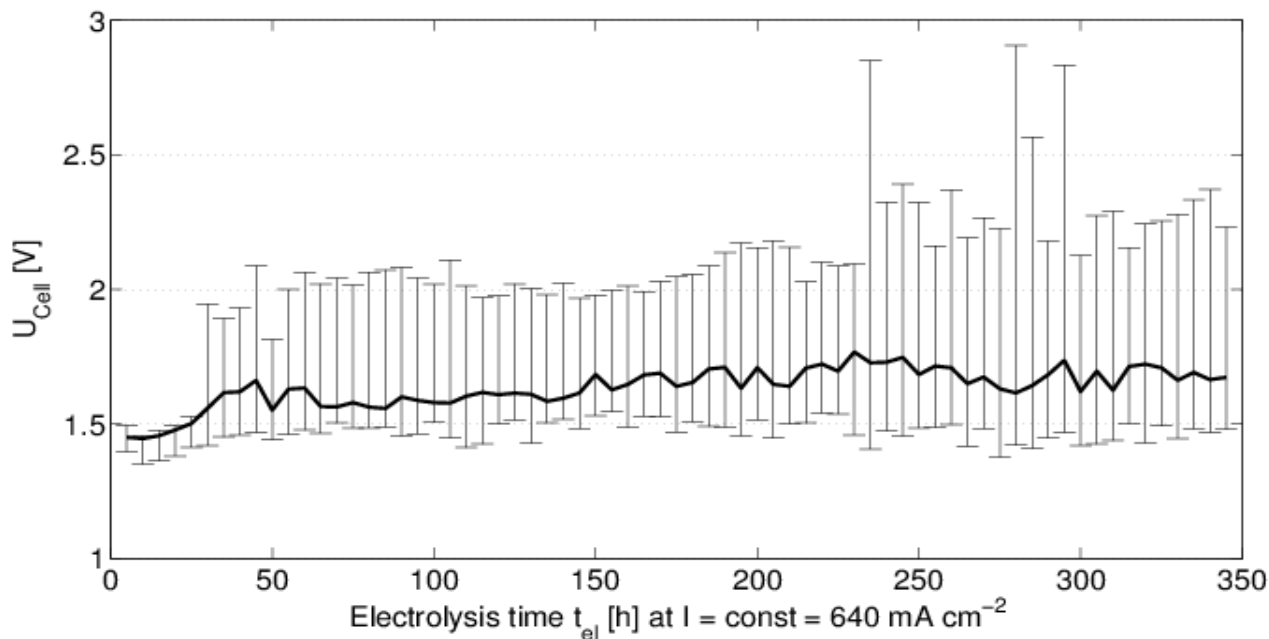


Figure 40 Development of the 5 h average of the applied cell voltage along the min and max values over the entire measurement period of 345 hours with a constant current density of  $640 \text{ mA cm}^{-2}$ , at  $250 \text{ }^\circ\text{C}$  and  $40 \text{ bar}$ .

A fast Fourier transformation FFT of the raw data was performed in order to analyse if the peaks had one or more specific repetition frequencies or if their periodicity varied randomly. It was concluded that the peaks varied randomly. This may be interpreted as an effect of formation of probably big gas bubbles that stayed on the hydrogen electrode for stochastically varying length of time.

### 5.3.7. Summary

Comparison of the results from the high temperature and pressure measurements to the results from the measurements in the low temperature measurement setup displayed in Figure 34, gives an impression on how significantly the current density of an alkaline electrolysis cell can be increased by increasing the temperature. The analysed Raney-nickel foam electrode obtained a current density of  $40 \text{ mA cm}^{-2}$  at an applied cell voltage of  $1.75 \text{ V}$  and a temperature of  $100 \text{ }^\circ\text{C}$ . Cell 2 and 3a from Figure 35 reached current densities of  $1.57 \text{ A cm}^{-2}$  and  $2.0 \text{ A cm}^{-2}$  at temperatures and pressures around  $250 \text{ }^\circ\text{C}$  and  $40 \text{ bar}$ . The Raney-nickel electrode reached a current density of  $200 \text{ mA cm}^{-2}$  at a relatively high cell voltage of  $2.24 \text{ V}$  at  $100 \text{ }^\circ\text{C}$ . It should be stressed out that neither the Raney-nickel electrode nor the low temperature measurement system has been optimized. Furthermore, it is clear that a significant improvement of the obtained current densities is obtained in the high temperature measurements by comparing to literature data. Divisek et al. (1988) reached a current density  $400 \text{ mA cm}^{-2}$  at a cell voltage of  $1.55 \text{ V}$  and a temperature of  $100 \text{ }^\circ\text{C}$  on a Raney-nickel cell with both electrodes made of Raney-nickel. This is among the best reported in the literature for alkaline electrolysis, but less than half of the performance obtained in this project at  $250 \text{ }^\circ\text{C}$  and  $40 \text{ bar}$ .

Thus, it was demonstrated that increasing the operation temperature of an alkaline electrolysis cell can reduce the losses significantly, thereby increasing the electrical efficiency and decreasing the hydrogen production costs. Operation at elevated pressures can furthermore reduce the investment costs. Measurement systems were designed and constructed to conduct electrochemical measurements at temperatures up to 250 °C and a pressure of 95 bar.

### 5.3.8. List of publications of the project from DTU Energy Conversion

1. Frank Allebrod, "High temperature and pressure alkaline electrolysis", PhD thesis, DTU Energy Conversion, November 2012. The thesis will be available on the DTU web after defense and acceptance, which is scheduled to take place in January 2013. A printed copy is available for perusal at the main supervisor, Mogens B. Mogensen, DTU Energy Conversion.
2. Frank Allebrod, Christodoulos Chatzichristodoulou, Pia Lolk Mollerup, Mogens Bjerg Mogensen, "Electrical conductivity measurements of aqueous and immobilized potassium hydroxide", *International Journal of Hydrogen Energy*, **37** (2012) 16505 – 16514.
3. Frank Allebrod, Christodoulos Chatzichristodoulou, Mogens B. Mogensen, "Alkaline Electrolysis Cell at High Temperature and Pressure of 250 °C and 42 bar", submitted to *Journal of Power Sources* 2012, accepted with conditions.
4. Frank Allebrod, Christodoulos Chatzichristodoulou, Pia Lolk Mollerup, Mogens Mogensen, "High Performance Reversible Electrochemical Cell for H<sub>2</sub>O Electrolysis or conversion of CO<sub>2</sub> and H<sub>2</sub>O to Fuel", Patent Application nr. EP12164019.7, Date of filing: 13/04/2012.

## 5.4. Results on improved electrodes

Work package 1 has covered the development of three different electrode tracks. The aim of this WP has been to cover the two first objectives of the project, to increase electrode efficiency to more than 88% at a current density of 200 mA /cm<sup>2</sup> as well as increase the operation temperature to more than 100 degree Celsius to make the cooling energy more valuable. The findings from the three electrode technology tracks are summarized in the following.

From the beginning only electroplating and the atmospheric plasma spray technology have been considered as competing technologies in a pre-commercial scale. The HTP track is still on a research stage and further development is needed before the electrode is implemented in a cell that will be an option for commercial use.

### 5.4.1. Electroplating

During the presented Ph.D. study, at DTU-ME a new type of electrodes, suitable for industrial alkaline water electrolyzers, has been developed. The electrodes are produced by magnetron sputtering a thin film of aluminium onto a nickel or nickel plated substrate. Hereafter, the aluminium is interdiffused into the nickel surface, by heating, and several intermetallic phases between Al and Ni are formed. Lastly, aluminium is selectively leached from one of the intermetallic phases on the surface and high porous nickel electrode is formed.

The structure of the developed electrodes has been characterised via high resolution scanning electron microscopes, revealing large actual surface area with pores down to 20 nm.

Consistent electrochemical measurements show that the developed electrodes need 450 mV less voltage for decomposing water into hydrogen and oxygen compared to smooth nickel electrodes, in 1 M KOH at 25 °C and 1 atm.

Durability test in an electrolysis stack for 9,000 hours indicated no serious mitigation in the electrode efficiency during the test period. The efficiency of the electrolysis stack was measured to be around 78-79 % compared to the higher heating value (HHV) at 65 °C. It should be mentioned that the electrolysis stack was of an old version and some efficiency loss was caused by the stack itself and not by the electrodes. The same stack was tested at H2College at a temperature of 74.4 °C. Here an efficiency of 86.5% was obtained.

#### **5.4.2. Atmospheric Plasma Spray**

Quite early in the project conducted by FORCE Technology, it was shown that highly efficient cathode coatings meeting the goal of 88 % efficiency could be produced by Atmospheric Plasma Spraying (APS). At the same time, FORCE Technology established a test concept for characterising the electrode coatings that verified APS coatings as fully comparable or better than those described in the literature. Both efforts placed the project right on track from the beginning.

Further developments of the APS coatings led to additional improvements in stability of substrate, adhesion to substrate, spraying parameters and optimisation of coating thickness.

Larger electrodes in many shapes were provided for the pilot test stacks with promising results, though the reproducibility was not necessarily evident. Near the end of year two, only marginal improvements were made on the NiAl coatings for the cathode. At this stage, the cathode side was considered nearly or fully developed as evidenced by the impressive efficiency reported for the pilot cells (97 %). The subsequent development of coatings for the anode side did not provide the desired results, but gained important insight about possible future process routes.

The developed NiAl electrodes produced by APS have made major steps forward to be suitable for large-scale production. However further long-term test for verifying the durability and life time still have to be conducted. Furthermore price reductions are still needed to make the technology competitive. This requirement might be met by going for a large scale production. However, this will require investments and establishment of a company outside FT auspices.

#### **5.4.3. HTP electrodes**

In the Ph.D. study at DTU-EC, comparison of the results from a high temperature and pressure measurements with the results from the measurements in a low temperature setup have shown how significantly the current density of an alkaline electrolysis cell can be increased by increasing the temperature. Analyses have shown Raney-nickel foam electrode can obtain a current density of 40 mA cm<sup>-2</sup> at an applied cell voltage of 1.75 V and a temperature of 100 °C. Further the Raney-nickel electrode has

reached a current density of  $200 \text{ mA cm}^{-2}$  at a relatively high cell voltage of  $2.24 \text{ V}$  at  $100 \text{ }^\circ\text{C}$ . In comparison current densities of  $1.57 \text{ A cm}^{-2}$  and  $2.0 \text{ A cm}^{-2}$  have been reached when temperatures around  $250 \text{ }^\circ\text{C}$  and pressures at  $40 \text{ bar}$  have been applied to the HTP electrode. It should be stressed that neither the Raney-nickel electrode nor the low temperature measurement system has been optimized. Furthermore, from literature data it is clear that a significant improvement in current densities is obtained in a high temperature scenario. Divisek et al. (1988) reached a current density  $400 \text{ mA cm}^{-2}$  at a cell voltage of  $1.55 \text{ V}$  and a temperature of  $100 \text{ }^\circ\text{C}$  on a Raney-nickel cell with both electrodes made of Raney-nickel. This is among the best reported in the literature for alkaline electrolysis, but less than half of the performance obtained in this project at  $250 \text{ }^\circ\text{C}$  and  $40 \text{ bar}$ .

Thus, the project has demonstrated that increasing the operation temperature of an alkaline electrolysis cell can reduce the losses significantly, thereby increasing the electrical efficiency and decreasing the hydrogen production costs. Operation at elevated pressures can furthermore reduce the investment costs. However as these results are obtained in a research lab on a cell measuring  $1 \text{ cm}^2$ , further developments are required to demonstrate the findings in a full scale cell, stack and system.

#### **5.4.4. Conclusion**

The results obtained in this work package show that the electroplating track on the short term gives the most promising performance when combining durability, lifetime, efficiency and price.

For the APS method higher cell efficiencies has been reached, however long term test on durability is still needed as well as further reduction in price is required.

Finally, the HTP track has shown that elevated process temperature causes remarkably higher current density entailing higher cell efficiency.



## 6. Higher operation pressure (WP 3)

The goal set for the second generation electrolyser system, has been to generate 30 bar pressure in the cell stack. Operating at elevated pressure have several advantages, but also proves to have some challenges. In this work package solutions for overcoming the challenges has been developed.

When water is split by electrolysis, hydrogen is naturally generated at a very high pressure. If the generated hydrogen is contained, it is possible to generate compressed hydrogen directly from the cell stack, without spending additional electricity. This is a great advantage, as the hydrogen can be pressurized up to 30 bar, without using a conventional compressor, which is both energy consuming, and costly. While some applications will need further compression for storing the hydrogen, it will be possible for many applications to work completely without a compressor, greatly simplifying and improving the overall system.

Another great advantage of high pressure electrolysis is the reduced size of tubing and components. Compared to hydrogen at atmospheric pressure the reduced volume of the compressed hydrogen provide a possibility to increase the capacity or reduce the size of the components by a factor equal to the pressure ratio, and still retain the same flow rates and roughly the same pressure drops. This enables the electrolyser system to be designed with a significantly smaller footprint than equivalent atmospheric systems. The reduction of components size provides a possibility to modularize the electrolyser concept, as well as reducing the price of the individual components.

One of the drawbacks of high pressure hydrogen electrolysis is increasing demands on materials and stack design, as the electrolysis stack will need to be manufactured primarily from a nonconductive material which is chemically stable against hot KOH, H<sub>2</sub> and O<sub>2</sub>, and still satisfy the mechanical requirements for containing electrolysis under 30 bar.

To accommodate the higher pressure, the stack has been designed as a cylindrical pressure vessel, with each cell having a cell “wall” sufficiently thick, to resist the high pressure and sealed with O-rings for perfect sealing at high pressures.

For a more detailed description of the stack design, see chapter 7.

Another challenge for high pressure electrolysis has been equalisation of the H<sub>2</sub> and O<sub>2</sub> pressure. As with electrolysis under atmospheric pressure, it is important to control the pressure on the H<sub>2</sub> and O<sub>2</sub> side of the electrolyser, to ensure that no mixing of gasses can occur. At atmospheric pressure the system is controlled passively with gravity ensuring the system stays in balance, hence no pressure difference can drive gas to cross the diaphragm or cause emptying or flooding of the separator or scrubber vessels.

At elevated pressures however, it becomes increasingly difficult to control the pressures within milli-bars, which is necessary for maintaining the water



levels of the separator and scrubber vessels in equilibrium.

To solve this problem, a special equilibrium valve has been developed to mechanically control that the pressure of the H<sub>2</sub> at all times equals the O<sub>2</sub> side . The valve was designed in such a way, that even a slight difference in pressure between the sides, causes the under-pressured side to close. Thus pressure will be build up until it is equal to the over-pressured side. This regulation is constant and gradual, and will maintain the pressure difference between the sides within milli-bars.

## 7. Improved electrolysis stack architecture (WP 4)

The primary goal of WP4 has been to develop an electrolyser stack concept suitable for mass production, while still solving the technical challenges when designing a high pressure alkaline electrolyser stack.

The challenges for construction of a high pressure alkaline electrolyser stack are mechanical strength, electrolyte and gas flow, stray currents and galvanic corrosion.

The first design decision after deciding to develop a high pressure electrolysis stack, was to decide on a zero gap or non-zero gap design. The advantages of a zero gap design, is the improved efficiency of the electrolyser, because of a reduced distance between electrodes. However a zero gap design is also very costly, primarily because the additional materials and production costs for zero gap electrodes.

When operating an electrolyser at a higher pressure, it is possible to reduce the distance between electrodes, because of smaller volumes of gas being released. This factor is very important for the design of a high pressure alkaline electrolyser, because it enables the use of the much simpler non-zero gap design. For this design to be viable however, it is necessary to keep the active area of each electrode sufficiently small, to keep the volumetric ratio of gas to electrolyte low and to maintain a high conductivity in the electrolyte, even at the top of the electrolysis cells where gas bubbles will naturally accumulate.

It was from these considerations, the concept of a “low gap”, low diameter, high pressure and high cell number electrolyser stack was born.

For the scope of mass production and cost reduction, this design philosophy is also ideal, because it allows the use of only very few different parts, with a relatively small size, in large quantities.

Locked in to this design philosophy, it was now necessary to consider the next design constraint on the electrolyser stack: The mechanical strength.

To achieve a sufficiently high mechanical strength of the electrolyser stack, several approaches was researched, and it was settled on using a high strength polymer for the bulk cell material. The cells have therefore been designed with a sufficient wall thickness to be tested up to 40bar.

The great advantage of using a polymer material is the possibility for mass production by injection moulding. However, great care has been taken when selecting material for injection moulding of cell frames, as reinforcements and flow fronts during moulding are very important for the overall strength of the material.

Related to the material strength of the cell stack, is also the thermal expansion of the cell frames with increasing temperature. Because of the uneven expansion of the cell frames and the tie rods of the electrolyser, it is necessary to use disc springs to allow thermal expansion of the electrolysis stack.

In an electrochemical system an electric circuit is formed by making a bridge through an electrolyte. For the case of alkaline water electrolysis, the circuit is formed by transporting OH<sup>-</sup> from the cathode to the anode, releasing H<sub>2</sub> and O<sub>2</sub> respectively.

This mechanic however, results in some technical difficulty when it comes to designing an alkaline electrolysis stack, because an electrolyser of the bipolar design has shared manifolds. Each electrode can here see all other electrodes through the ports and manifolds of the system, which result in unintended currents through ports and manifolds.

These currents are commonly named either stray currents, shunt currents or leak currents.

Dimensioning for stray currents was part of the initial considerations, as a design was proposed with long ports with a low cross sectional area. However, during experiments of the stack, it was understood that the stray currents was significantly increased with a higher cell number than what was expected from initial calculations, even though steps was taken to reduce the effect during cell design.

The challenges of limiting stray currents was more comprehensive than initially expected and the result is that alternative methods for reducing stray currents in high cell number stacks has been designed for testing in future generations of the high pressure alkaline electrolyser stack. And a more detailed understanding of the stray current phenomena has been used to develop more accurate computer models.

## 8. Corrosion resistant materials (WP 5)

If hydrogen is to be produced at increased temperature, pressure and stack voltage, it requires that the electrolyser can withstand the aggressive alkaline media under those severe conditions. A design life of more than 10 years is a challenge in terms of materials. The corrosion mechanisms of metallic materials have previously been studied under similar conditions, and literature data and experience were collected to identify critical risks of corrosion and stress corrosion cracking. Corrosion may be a problem for the electrolyser components both in terms of poisoning the electrodes (iron contamination) and structural risk. This reduces the options for metallic materials to primarily nickel-based alloys, if the cell should run at the defined conditions (30 % KOH, 100 °C, 20 bar). If austenitic stainless steels are to be used, the conditions must be less severe. The data were applied in the design of experimental cells.

Summary of corrosion tests in autoclave at 120 °C in 25 % KOH for 14 days.			
Material type	Pass/Fail	Comments	Application
PPS	Fail	Glass fibres dissolved, cracks and dimensional and weight change	Cell frame
PA	Fail	Decomposed	Cell frame
PEI	Fail	Decomposed	Cell frame
PPS	Fail	Blisters	Cell frame
PFA	Pass	Slight discoloration	Cell frame
PEEK	Pass	No sign of degradation	Cell frame
PEEK+CA	Pass	No sign of degradation	Cell frame
PESU	Pass	Small blister at cut face	Cell frame
PS	Pass	No sign of degradation*	Diaphragm
PS	Pass	Slight weight gain	Diaphragm
PS + Zr oxide (90C)	Fail	Decomposed*	Diaphragm
PS + Zr oxide (120C)	Pass	No sign of degradation*	Diaphragm
PS + Zr oxide (500)	Pass	No sign of degradation	Diaphragm
PS + Zr oxide (550)	Pass	No sign of degradation	Diaphragm

Table 5 Summary of corrosion tests in autoclave at 120 °C in 25 % KOH for 14 days.

\*7 days test only as autoclave cracked by stress corrosion cracking in test.

The initial literature survey and the first tests at H2College also indicated that the chemical resistance of polymers presented a greater challenge than anticipated, and that test data from commercial suppliers were insufficient to model the conditions in the electrolyser. The alkali resistant polymers (e.g. Teflon) are

costly and the search for cheaper alternatives turned into a major aim. The progress of the project therefore required corrosion testing and examination of polymers to find alternative durable membrane and gasket materials. A number of different tests were run under accelerated conditions and the degradation mechanism was examined. The results of standardised tests are summarised in Table 5. Consequently, the project has involved corrosion testing and examination of polymers to greater extent than originally planned at the detriment of long-term testing of electrodes (WP 1.8), which has been limited.

Inspiration for the future materials selection in electrolysers is now available by the combined experience from the experimental work and literature.

## 9. Modular design for easy up scaling (WP 6)

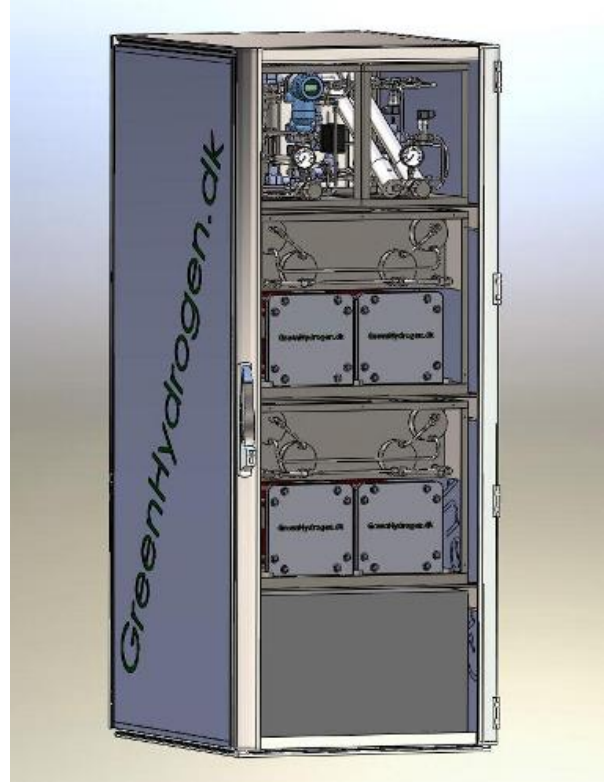
One of the strong visions for the second generation electrolyser concept was to develop a modular system with several standardized components, to make it possible to deliver a wide range of specification and features to the customer depending on the application.

The use of a modular system is also aimed at making service faster and easier, by making it possible to replace defect modules directly on site to decrease the downtime. And also centralize the repair of defect modules to the company workshop, greatly reducing the need for mobile tools and technicians.

A great effort has been put into analysing the electrolysis system to determine how the different components could be split onto modules. The end result is that following modules have been designed.

- Electrolyser module
- Deoxer Module
- Dryer Module
- Water Treatment Module
- Power supply and Control unit
- Rack mount

The Electrolyser, Deoxer and Dryer module have been designed and manufactured from scratch, where the power supply and control unit, water treatment module and rack mount have been manufactured from existing and standardized components.



### 9.1. Electrolyser module

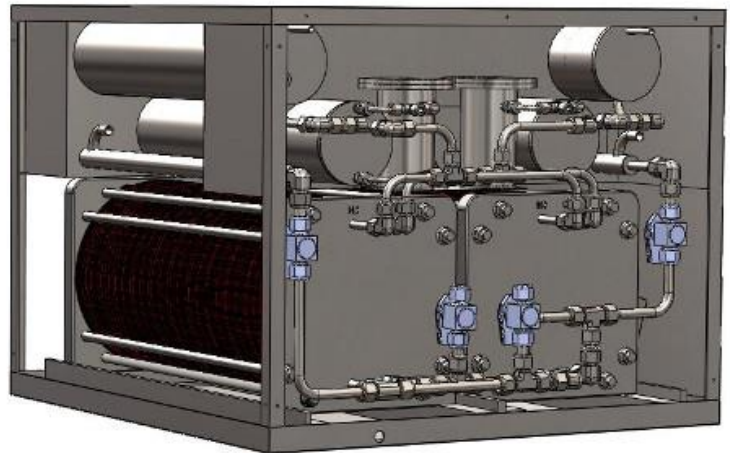
The purpose of this module is to convert water into hydrogen by applying a DC current to a water based electrolyte. The splitting of the water occurs in the stack component, where electrolyte (lye, KOH) is continuously fed into a channel in the bottom. The stack consists of a number of cells, where the H<sub>2</sub> and O<sub>2</sub> production occurs. The cells are all connected by channels, where a common H<sub>2</sub> and O<sub>2</sub> outlet is connected to a H<sub>2</sub> and an O<sub>2</sub> separator vessel. During electrolysis, the electrolyte will be filled with small gas bubbles. These bubbles will reduce the density of the electrolyte, and thereby cause a circulation, since the density of the lye in the return flow is higher. The electrolyte/gas mixture is thus pumped into the separator vessels.

In the separator vessels, the gases are separated from the electrolyte, and afterwards the hydrogen and oxygen is scrubbed with demineralized water from the water supply to remove residual amounts of lye from the gas. After separation, the gasses exits the module.

The control concept for the electrolysis module is based on an equalization valve that only allows flow of both gasses, as long as the hydrogen and oxygen have equal pressure. A pressure drop in one of the gasses will result in the valve blocking the flow, until pressures become equal again. This will ensure that the gasses can't pass through the diaphragm and mix with each other.

A nitrogen purge channel is connected to both separator vessels in order to purge the system during startup and when service is needed.

The water consumed by the electrolysis process is refilled into the scrubber compartments of the separator vessels. There will thus be a constant refill with demineralized water from this compartment into the separators, which ensures the water supply for the electrolysis.



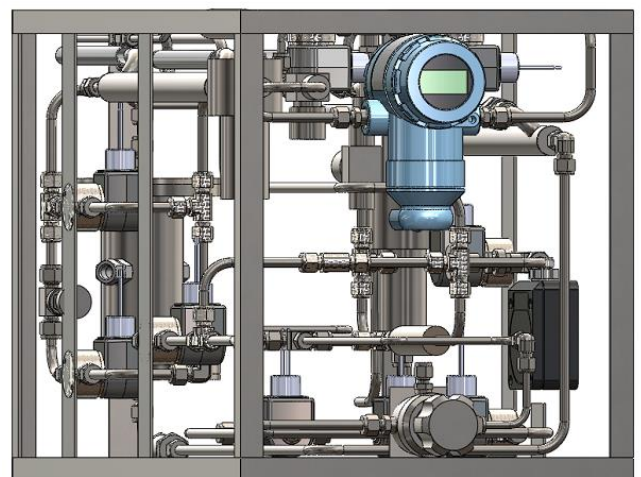
## 9.2. Deoxer Module

The primary function of this module is to remove oxygen from the hydrogen by catalytically burning the oxygen and secondarily drain water from the system.

The wet hydrogen is initially cooled and excess water is drained, to avoid liquid water from causing corrosion within the deoxer and inhibit the catalytic process. The hydrogen is then preheated by the ambient temperature in the rack before entering the catalytic burner (Deoxer),

When the condensed water is taped a small amount of hydrogen is released to the atmosphere at the same time.

The deox module is also responsible for controlling the purity of the oxygen and hydrogen for safety reasons, to avoid generation of explosive gas mixtures.





### 9.3. Dryer Module

Drying is accomplished by leading the product gas through a zeolite that adsorbs water vapour, drying the gas down to a dew point of -80C.

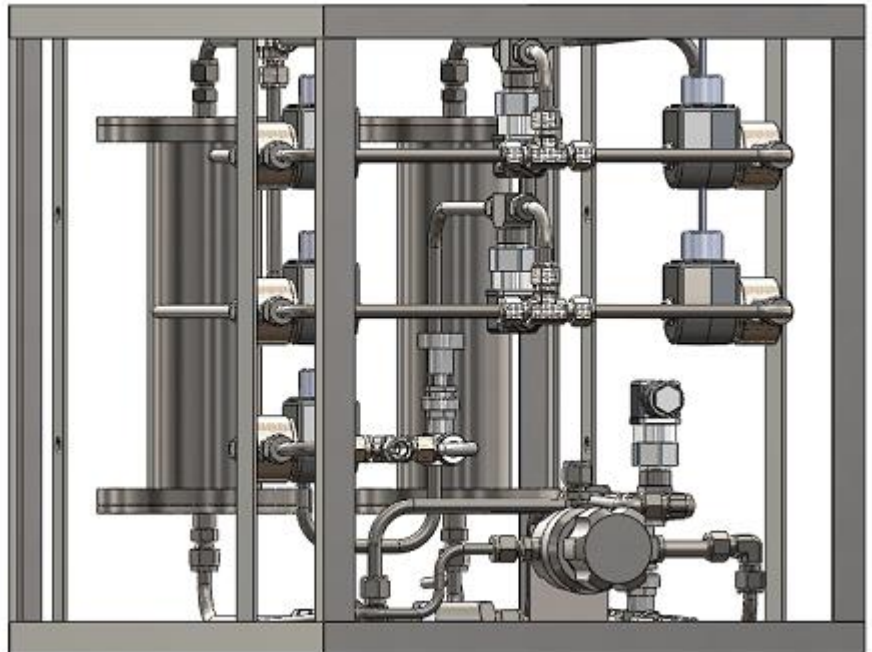
The zeolites are slowly saturated with water, and will therefore need regeneration.

Regeneration is done by utilizing a dual drying system, where one dryer dries the product gas, while the other dryer regenerates.

To regenerate a dryer, some of the dry product gas is led back through the dryer at low pressure, to carry away desorbing water from the zeolite. (the zeolite cannot contain much water at low pressure, and thus the water is desorbed.)

The wet regenerated gas is then vented to the atmosphere resulting in loss of overall system efficiency. The amount of gas needed for regenerating the dryer, is equal to the pressure ratio between the absorption pressure and the desorption pressure. Hence the higher pressure in the cell stack the less gas is needed for regeneration.

This loss of overall efficiency is not desired for systems that do not depend on hydrogen with very low water content. The dryer is therefore an optional module for these applications.



### 9.4. Water Treatment Module

This module contains the water treatment for the system.

Because water is split in the electrolyser, water will continuously need to be fed to the electrolyzer module. Which means any impurities in the water will increase in concentration during electrolysis. Some impurities, especially Cl have very damaging effects on the electrodes and it is therefore important to purify the water before it enters the system.

The water is led through a mix-bed ion exchanger in order to achieve a conductivity between 0,1-1 microSiemens. Depending on the water supply at the site, it can be necessary to implement a reverse osmosis unit for pre-treating the water before leading it into the mix-bed ion exchanger.

To feed the water into the pressurized electrolyser, the water is pressurized with a pump and led into a buffer vessel.

## **9.5.Power supply and Control unit**

The power supply was built as simple as possible and consist of a number of purchased AC/DC converters. The control unit is based on standard PLC controls.

This solution was selected because many good products are already available, and the area of power supply has not been the focus of this project.

The power supply and control system was for the H2 College electrolyser placed in a separate compartment for safety reasons.

## **9.6.Rack Mounted Electrolyser**

The goal was to design the electrolysis system so it would fit into standardized racks, to standardize the footprint measurements, and ease installation requirements.

This goal was achieved, so the only requirement currently, is available floor space, electricity, water, and pipes for hydrogen, oxygen and ventilation.

On top of the rack is mounted a blower, to apply constant suction to the electrolyser during operation, so to ensure any potential leak cannot build up to create an explosive atmosphere.

The end goal to be able to fit up to 8 Nm<sup>3</sup> electrolyser capacity into one rack (though currently the power supply and controls have been placed into a separate rack) is firmly believed possible, by fitting the controls and power supply into the bottom of the electrolyser rack, once the development leaves the prototype stage.

## 10. Demonstration (WP7)



Image 1: Electrolyser building at H2 college

### 10.1. Building and Installation

For containing the electrolyser and showcase hydrogen technology, a house was built in conjunction with the 66 H2 college houses. The electrolyser system was installed in winter 2010, with the entire project finalized early spring 2010. Once the ground thawed and it was possible to dig down the connecting pipe from the electrolyser building to the H2 college houses the plant was ready to deliver hydrogen to the fuel cells.

The installation of the electrolyser system was as simple as the modules had already been assembled from the workshop, so installation was limited to fixing the modules in the rack, connecting power, water, gas pipes and ventilation, and filling KOH to the electrolyser module.

Because of the prototype nature of the electrolyser, the controls for the system had not been finalized before the installation, so for the case of H2 college project, the commissioning of the plant was performed

on site. For future plants however, the commissioning will take place in the workshop, with only minimal adjustments if any, needing to be done one the site.



Image 2: Electrolyser system and storage tank

## 10.2.Measurement Results

### 10.2.1. Stack efficiency

A number of measurements were performed on the system installed in H2College, showing a stack efficiency of 86.5% at a current density of  $177\text{mA}/\text{cm}^2$  and a temperature of  $74.4\text{ }^\circ\text{C}$  at the hydrogen outlet.

### 10.2.2. System Efficiency

There have not been any measurements of the overall system efficiency

### 10.2.3. Total production hours

After installation the electrolyser system is estimated to have run roughly 2000h

### 10.2.4. Gas purity

The purity of the gas was testes before entering the deoxer to 0,3% oxygen in hydrogen, which is more than 10 times lower than the critical 4%.

### **10.2.5. Cooling**

The stack was not actively cooled, as passive cooling of the stack was sufficient to keep it at low temperatures. Conversely, it was required to insulate the system to achieve desired operating temperatures.

The cooling of product gas in the deox module have worked as intended, as no condensation of water has been detected after the deox module. For this reason it is assumed that it is not necessary to use a dryer module in applications where no additional compression is required.

## **10.3.Demonstration**

The demonstration of the second generation alkaline electrolyser is considered a success for several reasons. While not all technical goals were reached, the research and development in the project have resulted in some very good solutions for most of the challenges in high pressure alkaline electrolysis.

The concept of a rack mounted electrolyser was proven viable, and all critical aspects of the modularisation have been covered.

What H2 College demonstrates is therefore more than the development of a small size electrolyser, but it is a leap from developing electrolyser systems as a plant, to developing electrolyser systems as a product suitable for mass production.

## 11. List of publications

The findings of the project have been communicated in different ways. The following list embraces publications as articles in international journals as well as presentations and posters on national and international conferences.

*'Modelling electrolyte conductivity in a water electrolyzer cell'*, Michael Caspersen<sup>(a)</sup>, Technical University of Denmark, Julius Bier Kirkegaard<sup>(b)</sup>, Niels Bohr Institute, University of Copenhagen, *International Journal of Hydrogen Energy - Volume 37, Issue 9, May 2012, Pages 7436–7441*

*'Development of durable and efficient electrodes for large-scale alkaline water electrolysis'*, Cecilía Kjartansdóttir, [cckj@mek.dtu.dk](mailto:cckj@mek.dtu.dk), Technical University of Denmark, Lars Pleth Nielsen, [lpn@teknologisk.dk](mailto:lpn@teknologisk.dk), Danish Technological Institute, Per Møller, [pm@mek.dtu.dk](mailto:pm@mek.dtu.dk), Technical University of Denmark, *Submitted to International Journal of Hydrogen Energy January 31 2013.*

*'2nd Generation Alkaline Electrolysis for Hydrogen Production'*, Cecilía Kjartansdóttir, [cckj@mek.dtu.dk](mailto:cckj@mek.dtu.dk), Technical University of Denmark, Lars Pleth Nielsen, [lpn@teknologisk.dk](mailto:lpn@teknologisk.dk), Danish Technological Institute, Per Møller, [pm@mek.dtu.dk](mailto:pm@mek.dtu.dk), Technical University of Denmark, *Presented at the Metallurgisymposium, Roskilde on June 9 2011.*

*'Electrodes with good durability for alkaline water electrolysis'*, Cecilía Kjartansdóttir, [cckj@mek.dtu.dk](mailto:cckj@mek.dtu.dk), Technical University of Denmark, Lars Pleth Nielsen, [lpn@teknologisk.dk](mailto:lpn@teknologisk.dk), Danish Technological Institute, Per Møller, [pm@mek.dtu.dk](mailto:pm@mek.dtu.dk), Technical University of Denmark, *Poster presentation at World Hydrogen Energy Conference 2012, Toronto Canada June 2012*

*'Electrolysis plants heat balance'*, Lars Yde, [LarsY@hjh.au.dk](mailto:LarsY@hjh.au.dk)  
*Presentation at SYMPOSIUM on Water electrolysis and hydrogen as part of the future Renewable Energy System, DTU, Risø Campus*

*'Atmospheric plasma spraying of electrodes for conversion of electricity to hydrogen by high temperature alkaline electrolysis of water'*  
Peter Tommy Nielsen, [PTN@force.dk](mailto:PTN@force.dk), Troels Mathiesen, Jens Klæstrup Kristensen, Lisbeth Hilbert, FORCE Technology Denmark, Lars Yde, HIRC  
*Presentation and proceedings at International Thermal Spray Conference 2011, Hamburg September 2011*

*'Electrochemical characterisation of atmospheric plasma spray coatings for water electrolysis'*  
Troels Mathiesen, [TRM@force.dk](mailto:TRM@force.dk), Lisbeth Hilbert, Peter Tommy Nielsen, FORCE Technology Denmark  
*Poster presentation at Symposium: Water Electrolysis and hydrogen as a part of the future Renewable Energy System, Copenhagen May 2012. Also presented at DEF Electrochemical Science & Technology 2012, October 2012*

*'High Temperature and pressure alkaline electrolysis'*, Frank Allebrod, [fkal@dtu.dk](mailto:fkal@dtu.dk), Technical University of Denmark, Sune D Ebbesen, [sueb@dtu.dk](mailto:sueb@dtu.dk), Technical University of Denmark, Johan Hjelm, [johh@dtu.dk](mailto:johh@dtu.dk), Technical University of Denmark, Mogens Mogensen, [momo@dtu.dk](mailto:momo@dtu.dk), Technical University of Denmark, *Oral presentation at the Conference on Electrochemical Science and Technology, Roskilde, Denmark, October 1<sup>st</sup> 2009.*

*'Determining the Conductivity of Aqueous Electrolytes using the van der Pauw Method'* Frank Allebrod, [fkal@dtu.dk](mailto:fkal@dtu.dk), Technical University of Denmark, Pia Lolk Mollerup, [plmol@dtu.dk](mailto:plmol@dtu.dk), Technical University of Denmark, Mogens Mogensen, [momo@dtu.dk](mailto:momo@dtu.dk), Technical University of Denmark, *Poster presentation at the HyFC Academy summer school, Roskilde, Denmark, August 22<sup>nd</sup> – 26<sup>th</sup> 2010.*

*'Conductivity Measurements of Aqueous and Immobilized Potassium Hydroxide'* Frank Allebrod, [fkal@dtu.dk](mailto:fkal@dtu.dk), Technical University of Denmark, Pia Lolk Mollerup, [plmol@dtu.dk](mailto:plmol@dtu.dk), Technical University of Denmark, Mogens Mogensen, [momo@dtu.dk](mailto:momo@dtu.dk), Technical University of Denmark, *Poster presentation at the HyFC academy research school, workshop & annual meeting, Roskilde, Denmark, April 11<sup>th</sup> - 15<sup>th</sup> 2011.*

*'Electrolysis for Integration of Renewable Electricity and Routes towards Sustainable Fuels'*, Mogens Mogensen, [momo@dtu.dk](mailto:momo@dtu.dk), Technical University of Denmark, Frank Allebrod, [fkal@dtu.dk](mailto:fkal@dtu.dk), Technical University of Denmark, Jacob R. Bowen, [jrbo@dtu.dk](mailto:jrbo@dtu.dk), Technical University of Denmark, Christodoulos Chatzichristodoulou, [ccha@dtu.dk](mailto:ccha@dtu.dk), Technical University of Denmark, Ming Chen, [minc@dtu.dk](mailto:minc@dtu.dk), Technical University of Denmark, Sune D Ebbesen, [sueb@dtu.dk](mailto:sueb@dtu.dk), Technical University of Denmark, Christopher R. Graves, [cgra@dtu.dk](mailto:cgra@dtu.dk), Technical University of Denmark, Jonathan Hallinder, [jnhal@dtu.dk](mailto:jnhal@dtu.dk), Technical University of Denmark, Anne Hauch, [hauc@dtu.dk](mailto:hauc@dtu.dk), Technical University of Denmark, Peter Vang Hendriksen, [pvhe@dtu.dk](mailto:pvhe@dtu.dk), Technical University of Denmark, Peter Holtappels, [peho@dtu.dk](mailto:peho@dtu.dk), Technical University of Denmark, Jens Valdemar Thorvald Høgh, [jehq@dtu.dk](mailto:jehq@dtu.dk), Technical University of Denmark, S.H. Jensen, [shji@dtu.dk](mailto:shji@dtu.dk), Technical University of Denmark, Alberto Lapina, [alap@dtu.dk](mailto:alap@dtu.dk), Technical University of Denmark, Pia Lolk Mollerup, [plmol@dtu.dk](mailto:plmol@dtu.dk), Technical University of Denmark, Xiufu Sun, [xisu@dtu.dk](mailto:xisu@dtu.dk), Technical University of Denmark, *10<sup>th</sup> International Workshop on Large-Scale Integration of Wind Power into Power Systems as well as on Transmission Networks for Offshore Wind Farms, 2011, isbn: 978-3-9813870-3-2.*

*'Electrical conductivity measurements of aqueous and immobilized potassium hydroxide'*, Frank Allebrod, [fkal@dtu.dk](mailto:fkal@dtu.dk), Technical University of Denmark, [fkal@dtu.dk](mailto:fkal@dtu.dk), Christodoulos Chatzichristodoulou, [ccha@dtu.dk](mailto:ccha@dtu.dk), Technical University of Denmark, Pia Lolk Mollerup, [plmol@dtu.dk](mailto:plmol@dtu.dk), Technical University of Denmark, Mogens Mogensen, [momo@dtu.dk](mailto:momo@dtu.dk), Technical University of Denmark, *Proceedings of the International Conference on Hydrogen Production, ICH2P-11, Paper No 181ELE, June 19-22, 2011, Thessaloniki, Greece.*

*'Electrical conductivity measurements of aqueous and immobilized potassium hydroxide'*, Frank Allebrod, [fkal@dtu.dk](mailto:fkal@dtu.dk), Technical University of Denmark, Christodoulos Chatzichristodoulou, [ccha@dtu.dk](mailto:ccha@dtu.dk), Technical University of Denmark, Pia Lolk Mollerup, [plmol@dtu.dk](mailto:plmol@dtu.dk), Technical University of Denmark, Mogens Mogensen, [momo@dtu.dk](mailto:momo@dtu.dk), Technical University of Denmark, *International Journal of Hydrogen Energy, Volume 37, Issue 21, Pages 16505 – 16514, November 2012.*

*'High Performance Reversible Electrochemical Cell for H<sub>2</sub>O Electrolysis or Conversion of CO<sub>2</sub> and H<sub>2</sub>O to Fuel'*, Frank Allebrod, [fkal@dtu.dk](mailto:fkal@dtu.dk), Technical University of Denmark, Christodoulos Chatzichristodoulou, [ccha@dtu.dk](mailto:ccha@dtu.dk), Technical University of Denmark, Pia Lolk Mollerup, [plmol@dtu.dk](mailto:plmol@dtu.dk), Technical University of Denmark, Mogens Mogensen, [momo@dtu.dk](mailto:momo@dtu.dk), Technical University of Denmark, *patent Pending No. 12164019.7-2119, April 2012.*



*'FobAEC – Foam based Alkaline Electrochemical Cell for High Temperature and Pressure Alkaline Electrolysis'*  
Frank Allebrod, [fkal@dtu.dk](mailto:fkal@dtu.dk), Technical University of Denmark, Christodoulos Chatzichristodoulou,  
[ccha@dtu.dk](mailto:ccha@dtu.dk), Technical University of Denmark, Mogens Mogensen, [momo@dtu.dk](mailto:momo@dtu.dk), Technical University of  
Denmark, *Poster presentation at the Water electrolysis and hydrogen as part of the future Renewable  
Energy System symposium, Copenhagen, Denmark, May 10<sup>th</sup> - May 11<sup>th</sup> 2012.*

*'High temperature and pressure alkaline electrolysis cell'*, Frank Allebrod, [fkal@dtu.dk](mailto:fkal@dtu.dk), Technical University  
of Denmark, Christodoulos Chatzichristodoulou, [ccha@dtu.dk](mailto:ccha@dtu.dk), Technical University of Denmark, Mogens  
Mogensen, [momo@dtu.dk](mailto:momo@dtu.dk), Technical University of Denmark, *Oral presentation at the World Hydrogen  
Energy Conference 2012, Toronto, Canada, June 3<sup>rd</sup> - June 7<sup>th</sup> 2012.*

*'Alkaline Electrolysis Cell at High Temperature and Pressure of 250 °C and 42 bar'*, Frank Allebrod,  
[fkal@dtu.dk](mailto:fkal@dtu.dk), Technical University of Denmark, Christodoulos Chatzichristodoulou, [ccha@dtu.dk](mailto:ccha@dtu.dk), Technical  
University of Denmark, Mogens Mogensen, [momo@dtu.dk](mailto:momo@dtu.dk), Technical University of Denmark, *Journal of  
Power Sources, Volume 229, pages 22-31, May 2013.*

*'High Temperature and Pressure Alkaline Electrolysis'*, Frank Allebrod, [fkal@dtu.dk](mailto:fkal@dtu.dk), Technical University of  
Denmark, *PhD Thesis, Technical University of Denmark, Risø Campus, Roskilde, Denmark, submitted  
November 14<sup>th</sup> 2012 and defended February 28<sup>th</sup> 2013.*